

Non-asymptotic quantisation of spherically symmetric distributions

Luc Pronzato* and Anatoly Zhigljavsky†

May 14, 2026

Abstract

Zador’s celebrated theorem is a cornerstone of optimal quantisation, establishing both the weak limit of the empirical distribution of an n -point optimal quantiser in \mathbb{R}^d and the decay rate of the associated L_s -mean quantisation error. However, for large dimensions d , observing this asymptotic behaviour demands an astronomically large sample size n , which grows super-exponentially with d . Through a detailed analysis of the quantisation problem for spherically symmetric distributions, we demonstrate that for moderate n random quantisers uniformly distributed on a sphere of suitable radius R achieve exceptional performance. The expected distortion, expressed as a triple integral, can be computed with arbitrary precision, and the optimal radius R can be efficiently determined numerically. Leveraging results from extreme-value theory, we derive approximations for R , particularly in scenarios where n scales with d . Depending on the growth rate of n , R may either converge to zero or approach a limiting value R_∞ that is independent of s .

keywords: quantisation, distortion, spherically symmetric distribution, Zador’s theorem, extreme-value theory

1 Introduction

For μ a measure on $\mathcal{X} \subseteq \mathbb{R}^d$ (or a d -dimensional Riemannian manifold), with density φ and finite moment of order $s' > s \geq 1$, the (μ, s) -distortion on an n -point set $\mathbf{X}_n = \{\mathbf{x}_1, \dots, \mathbf{x}_n\} \in \mathbb{R}^{n \times d}$ is $D_{\mu,s}(\mathbf{X}_n) = \mathbb{E}_\mu\{\min_{i=1,\dots,n} \|U - \mathbf{x}_i\|^s\}$, where $U \stackrel{d}{\sim} \mu$. Zador’s celebrated theorem [13] states that the empirical distribution of an n -point optimal quantiser \mathbf{X}_n^* minimising $D_{\mu,s}(\mathbf{X}_n)$ converges weakly to the probability measure with density proportional to $\varphi^{d/(d+s)}$ as $n \rightarrow \infty$, and the normalised optimal (μ, s) -distortion $n^{1/d} D_{\mu,s}(\mathbf{X}_n^*)$ reaches asymptotically its minimum as $n \rightarrow \infty$. The normalisation by $n^{1/d}$ is essential, in the sense that these asymptotic considerations are not applicable if $n^{1/d}$ is not large enough. For large d , this requires astronomically large values of n to approach the asymptotic behaviour.

The purpose of this paper is to show that for μ spherically symmetric, random quantisers with a suitable spherically symmetric distribution can achieve exceptional performance. When n is large but $n^{1/d}$ is small, the best random quantisers we obtain are for designs \mathbf{X}_n uniform on a sphere $\mathcal{S}_{d-1}(R)$ with suitable radius R , and the variability of $D_{\mu,s}(\mathbf{X}_n)$ vanishes as n increases. Using extreme-value theory, we derive approximations for the radius R of \mathcal{S}_{d-1} and for the best expected (μ, s) -distortion. In the particular case $s = 2$, R is proportional to $\mathbb{E}_\mu\{\|U\|\}$ with

* (corresponding author) Laboratoire I3S, CNRS-Université Côte d’Azur, Sophia Antipolis, France, pronzato@i3s.unice.fr

† School of Mathematics, Cardiff University, UK, ZhigljavskyAA@cardiff.ac.uk

a constant depending only on n and d , and the best expected $(\mu, 2)$ -distortion is $\mathbb{E}_\mu\{\|U\|^2\} - R^2$; see Corollary 4.1. We then identify different asymptotic regimes where d increases and n grows with d . When μ possesses a norm-concentration property and concentrates on a sphere of radius r as $d \rightarrow \infty$, the optimal radius R of the random quantiser exhibits distinct behaviours depending on the growth rate of n relative to d : for a sub-exponential growth, $R \rightarrow 0$; for a super-exponential growth, $R \rightarrow r$; for an exponential growth $n = \lambda^d(1 + o(1))$, $R \rightarrow r\sqrt{1 - 1/\lambda^2}$; see Proposition 4.2. Overall, the paper provides a framework for generating nearly optimal quantisers in the large n and d situation for spherically symmetric distributions. Sequences of nested designs with low quantisation error can thus be efficiently generated, offering a compelling alternative to the classical greedy-packing algorithm for space-filling design (see, e.g., [11]). While this paper focuses exclusively on spherically symmetric distributions, the conclusion highlights that extending this approach to the more common case of quantising the uniform measure in the d -dimensional hypercube yields promising numerical results.

The paper is organised as follows. Section 2 introduces the key concepts used throughout the paper. It also derives an explicit integral expression of the expected (μ, s) -distortion of a random quantiser whose n points are independently identically distributed (i.i.d.) according to a spherically symmetric distribution \mathbb{P} . Section 3 examines three emblematic cases: (i) μ is uniform on the unit sphere, (ii) μ is uniform in the unit ball, and (iii) μ follows a multivariate spherically symmetric normal distribution. In the latter two scenarios, in addition to the case where \mathbb{P} is uniform on a sphere, we also analyse the cases where \mathbb{P} is uniform in a ball and where \mathbb{P} is a multivariate spherically symmetric normal distribution. Section 4 applies extreme-value theory to derive asymptotic results ($n \rightarrow \infty$) for random quantisers uniform on a sphere. The analysis is conducted in two scenarios: when μ is uniform on a sphere; when μ is spherically symmetric and satisfies a norm-concentration property, with the ball-uniform and normal distributions serving as key examples. Section 5 provides a brief conclusion to the paper.

We denote by $\mathcal{B}_d(r)$ the d -dimensional (closed) Euclidean ball with center $\mathbf{0}_d$ and radius r and by $\mathcal{S}_{d-1}(r)$ the d -dimensional Euclidean sphere with center $\mathbf{0}_d$ and radius r ; $\|\cdot\|$ is the ℓ_2 -norm.

2 Distance c.d.f., quantisation error and distortion

2.1 Definitions and basic properties

For any n -point set \mathbf{X}_n we denote by $d(\cdot, \mathbf{X}_n)$ the distance function defined by $\mathbf{x} \in \mathbb{R}^d \mapsto d(\mathbf{x}, \mathbf{X}_n) = \min_{\mathbf{x}_i \in \mathbf{X}_n} \|\mathbf{x} - \mathbf{x}_i\|$; ν denotes a probability measure on \mathbb{R}^d .

Definition 2.1. For \mathbf{X}_n a fixed n -point set in \mathbb{R}^d , the distance c.d.f. $F(\cdot; \mathbf{X}_n, \nu)$ is the c.d.f. of the random variable $d(U, \mathbf{X}_n)$ when U is distributed with ν :

$$F(t; \mathbf{X}_n, \nu) = \nu \left\{ U \in \bigcup_{i=1}^n \mathcal{B}_d(\mathbf{x}_i, t) \right\} = \nu\{d(U, \mathbf{X}_n) \leq t\}.$$

When $\mathbf{X}_n = \mathbf{R}_n$ is a random n -point set generated with some probability measure \mathbb{P} on $\mathbb{R}^{n \times d}$, we define the mean distance c.d.f. $F_n(\cdot; \mathbb{P}, \nu)$ of the random variable $d(U, \mathbf{R}_n)$ by $F_n(t; \mathbb{P}, \nu) = \mathbb{E}_\mathbb{P}\{F(t; \mathbf{R}_n, \nu)\}$.

If ν is the delta measure $\delta_{\mathbf{u}}$ concentrated at $\mathbf{u} \in \mathbb{R}^d$, the mean distance c.d.f. is simply $F_n(t; \mathbb{P}, \delta_{\mathbf{u}}) = \mathbb{P}\{d(\mathbf{u}, \mathbf{R}_n) \leq t\}$.

When \mathcal{X} is a compact subset of \mathbb{R}^d , we denote by $\text{CR}(\mathbf{X}_n) = \max_{\mathbf{x} \in \mathcal{X}} d(\mathbf{x}, \mathbf{X}_n)$ the covering radius of \mathbf{X}_n . If ν is equivalent to the Lebesgue measure on \mathcal{X} , $F(\cdot; \mathbf{X}_n, \nu)$ has a density on $[0, \text{CR}(\mathbf{X}_n)]$, which we denote by $f(\cdot; \mathbf{X}_n, \nu)$, and the essential supremum of the random variable $d(U, \mathbf{X}_n)$ equals $\text{CR}(\mathbf{X}_n)$. When ν is the uniform measure on \mathcal{X} , we simply denote the distance c.d.f. by $F(\cdot; \mathbf{X}_n)$: the random variable $d(U, \mathbf{x}_n)$ is supported on $[0, \text{CR}(\mathbf{X}_n)]$ and $F(\cdot; \mathbf{X}_n)$ contains all information about the filling of \mathcal{X} by \mathbf{X}_n . In particular, the γ -quantiles $q_\gamma(\mathbf{X}_n)$ of $F(\cdot; \mathbf{X}_n)$ provide useful space-filling characteristics. Assume that \mathcal{X} is connected and coincides with the closure of its interior. Then, the density $f(\cdot; \mathbf{X}_n)$ is strictly positive on $(0, \text{CR}(\mathbf{X}_n))$ and $q_\gamma(\mathbf{X}_n)$ is defined by

$$F[q_\gamma(\mathbf{X}_n); \mathbf{X}_n] = \gamma \quad \text{for any } \gamma \in (0, 1),$$

with $q_0(\mathbf{X}_n) = 0$ and $q_1(\mathbf{X}_n) = \text{CR}(\mathbf{X}_n)$.

Definition 2.2. *The L_s -mean quantisation error of a general probability measure μ on \mathbb{R}^d with finite s -th moment $\mathbb{E}\{\|X\|^s\}$ for a given n -point set \mathbf{X}_n is the $L_s(\mu)$ -norm of the distance function $d(\cdot, \mathbf{X}_n)$:*

$$E_{\mu,s}(\mathbf{X}_n) = \|d(\cdot, \mathbf{X}_n)\|_{L_s} = \left[\int_{\mathcal{X}} d^s(\mathbf{x}, \mathbf{X}_n) \mu(d\mathbf{x}) \right]^{1/s}, \quad s > 0.$$

The quantity $E_{\mu,s}^s(\mathbf{X}_n)$ is called the (μ, s) -distortion related to \mathbf{X}_n [9]. When $\mathbf{X}_n = \mathbf{R}_n$ is random, we define the expected (μ, s) -distortion as $D_{\mu,s}(\mathbb{P}) = \mathbb{E}_{\mathbb{P}}\{E_{\mu,s}^s(\mathbf{R}_n)\}$.

For any $s > 0$, the (μ, s) -distortion satisfies (see, e.g., [3, p. 150]):

$$E_{\mu,s}^s(\mathbf{X}_n) = \mathbb{E}_{\mu}\{d^s(U, \mathbf{X}_n)\} = s \int_0^\infty t^{s-1} [1 - F(t; \mathbf{X}_n, \mu)] dt. \quad (1)$$

The result is easily obtained when μ is such that $F(\cdot; \mathbf{X}_n, \mu)$ has a density $f(\cdot; \mathbf{X}_n, \mu)$. Indeed, by swapping the order of integration we get

$$\begin{aligned} \mathbb{E}_{\mu}\{d(U, \mathbf{X}_n)\} &= \int_0^\infty \tau f(\tau; \mathbf{X}_n, \mu) d\tau = \int_0^\infty \left(\int_0^\tau dt \right) f(\tau; \mathbf{X}_n, \mu) d\tau \\ &= \int_0^\infty \left(\int_t^\infty f(\tau; \mathbf{X}_n, \mu) d\tau \right) dt = \int_0^\infty [1 - F(t; \mathbf{X}_n, \mu)] dt. \end{aligned}$$

Now, for any $s > 0$, $G^{(s)}(\cdot; \mathbf{X}_n, \mu)$, defined by $G^{(s)}(t; \mathbf{X}_n, \mu) = F(t^{1/s}; \mathbf{X}_n, \mu)$ for any $t \geq 0$, is the c.d.f. of $d^s(U, \mathbf{X}_n)$, and we obtain

$$\mathbb{E}_{\mu}\{d^s(U, \mathbf{X}_n)\} = \int_0^\infty [1 - F(t^{1/s}; \mathbf{X}_n, \mu)] dt = s \int_0^\infty t^{s-1} [1 - F(t; \mathbf{X}_n, \mu)] dt.$$

Remark 2.1. *For any probability measure μ such that $\mathbb{E}\{\|X\|^{2s}\} < \infty$, the (μ, s) -distortion of an arbitrary n -point set \mathbf{X}_n can be approximated by its Monte-Carlo estimator $E_{\mu_N,s}^s(\mathbf{X}_n) = (1/N) \sum_{i=1}^N d^s(U_i, \mathbf{X}_n)$ where the U_i are i.i.d. with μ , and $E_{\mu_N,s}^s(\mathbf{X}_n)$ satisfies a classical central limit theorem:*

$$\sqrt{N} [E_{\mu_N,s}^s(\mathbf{X}_n) - E_{\mu,s}^s(\mathbf{X}_n)] \xrightarrow{d} \mathcal{N}(0, V(\mathbf{X}_n)), \quad N \rightarrow \infty,$$

where $V(\mathbf{X}_n) = E_{\mu,2s}^{2s}(\mathbf{X}_n) - E_{\mu,s}^{2s}(\mathbf{X}_n)$. When μ is supported on \mathcal{X} compact, $\text{CR}(\mathbf{X}_n) < \infty$ and a direct application of Hoeffding's inequality gives:

$$\text{for all } \alpha \in (0, 1), \quad \mu \{ |E_{\mu_N,s}^s(\mathbf{X}_n) - E_{\mu,s}^s(\mathbf{X}_n)| > \alpha \text{CR}(\mathbf{X}_n) \} < 2e^{-2N\alpha^2},$$

showing the exponentially fast concentration of $E_{\mu_N,s}^s(\mathbf{X}_n)$ to its mean $E_{\mu,s}^s(\mathbf{X}_n)$ as N increases. When μ has unbounded support, depending on its tail properties, other concentration inequalities can also be derived. \triangleleft

2.2 Quantisation error of random quantisers

Let $\mathbf{R}_n = \{\mathbf{x}_1, \dots, \mathbf{x}_n\}$ denote a random n -point set generated with a probability measure \mathbb{P} on $\mathbb{R}^{n \times d}$. Our objective is to choose \mathbb{P} so that the expected (μ, s) -distortion, $D_{\mu, s}(\mathbb{P})$ of Definition 2.2, is minimum.

From (1), we can write

$$D_{\mu, s}(\mathbb{P}) = s \int_{t \geq 0} t^{s-1} [1 - F_n(t; \mathbb{P}, \mu)] dt \quad (2)$$

where $F_n(\cdot; \mathbb{P}, \mu) = \mathbb{E}_{\mathbb{P}}\{F(t; \mathbf{R}_n, \mu)\}$ is the mean distance c.d.f. of Definition 2.1; that is, the c.d.f. of the random variable $d(U, \mathbf{R}_n)$ where both U and \mathbf{R}_n are random. The expected (μ, s) -distortion $D_{\mu, s}(\mathbb{P})$ is the (μ, s) -distortion for the c.d.f. $F_n(\cdot; \mathbb{P}, \mu)$. In this paper we focus on distortion and quantisation error, but we could have also considered the γ -quantiles of $F_n(\cdot; \mathbb{P}, \mu)$; see Remark 4.2. Note that Jensen inequality yields the following upper bound on the expected quantisation error: $\mathbb{E}_{\mathbb{P}}\{E_{\mu, s}(\mathbf{R}_n)\} \leq [D_{\mu, s}(\mathbb{P})]^{1/s}$ for $s \geq 1$.

By swapping the order of expectations, we get

$$\begin{aligned} F_n(t; \mathbb{P}, \mu) &= \mathbb{E}_{\mathbb{P}} \left\{ \mathbb{E}_{\mu} \left\{ \mathbb{1}_{\{\mathbf{u} \in \mathbb{R}^d: d(\mathbf{u}, \mathbf{R}_n) \leq t\}}(U) \right\} \right\} \\ &= \mathbb{E}_{\mu} \left\{ \mathbb{E}_{\mathbb{P}} \left\{ \mathbb{1}_{\{\mathbf{u} \in \mathbb{R}^d: d(\mathbf{u}, \mathbf{R}_n) \leq t\}}(U) \right\} \right\} \\ &= \mathbb{E}_{\mu} \{F_n(t; \mathbb{P}, \delta_{\mathbf{u}})\}, \end{aligned} \quad (3)$$

where $F_n(t; \mathbb{P}, \delta_{\mathbf{u}}) = \mathbb{P}\{d(\mathbf{u}, \mathbf{R}_n) \leq t\}$.

In the following, we consider random n -point set \mathbf{R}_n with i.i.d. points having the distribution \mathbb{P} , so that $\mathbb{P}(d\mathbf{x}_1, \dots, d\mathbf{x}_n) = \prod_{i=1}^n \mathbb{P}(d\mathbf{x}_i)$; we shall denote this distribution $\mathbb{P} = \mathbb{P}^{[n]}$. In Sections 2.3 and 2.4 we show that $F_n(t; \mathbb{P}^{[n]}, \mu)$ can be expressed in the form of a double integral when \mathbb{P} is spherically symmetric. This will rely on the following property which is true for any \mathbb{P} .

For any fixed $\mathbf{u} \in \mathbb{R}^d$, any $t \geq 0$ and any \mathbf{R}_n with i.i.d. points having the arbitrary distribution \mathbb{P} , we have

$$\begin{aligned} F_n(t; \mathbb{P}^{[n]}, \delta_{\mathbf{u}}) &= 1 - \prod_{j=1}^n \mathbb{P}\{\mathbf{u} \notin \mathcal{B}_d(\mathbf{x}_j, t)\} \\ &= 1 - \prod_{j=1}^n (1 - \mathbb{P}\{\mathbf{u} \in \mathcal{B}_d(\mathbf{x}_j, t)\}) = 1 - \left(1 - \mathbb{P}\{\|X - \mathbf{u}\| \leq t\}\right)^n, \end{aligned} \quad (4)$$

where $X \stackrel{d}{\sim} \mathbb{P}$.

The expression (4) indicates that the calculations of the mean distance c.d.f. $F_n(t; \mathbb{P}^{[n]}, \mu)$ and then of the expected (μ, s) -distortion require the calculation of the probability

$$\mathbb{P}\{\|X - \mathbf{u}\| \leq t\} = \mathbb{P}\{\mathbf{u} \in \mathcal{B}_d(X, t)\},$$

which depends on \mathbb{P} , \mathbf{u} and r . It is a consequence of the exchange of order of integration in (3) that we have to consider another distance c.d.f., where now \mathbf{u} is fixed and plays the role of a one-point quantiser, whereas X is random. Of course, this symmetry vanishes when considering random n -point sets, and the presence of n i.i.d. points is accounted for explicitly in (4). It is noticeable that this is the only place where the size n appears.

2.3 $\mathbb{P}\{\|X - \mathbf{u}\| \leq t\}$ when \mathbb{P} is spherically symmetric

By definition, the random vector $X = (X_1, \dots, X_d)$ is spherically symmetric if it can be represented as $X \stackrel{d}{=} R \cdot Z^{(d)}$, where $R = \|X\|$, $Z^{(d)} = (Z_1, \dots, Z_d)$ is uniformly distributed on the unit sphere $\mathcal{S}_{d-1}(1)$, and R and $Z^{(d)}$ are independent.

When \mathbb{P} is spherically symmetric the distribution of $\|X - \mathbf{u}\|$ for $X \stackrel{d}{\sim} \mathbb{P}$ only depends on $\|\mathbf{u}\|$ and d . This distribution is specified in Proposition 2.1 below. In the following, $\beta_{a,b}$ denotes a random variable with the Beta-density

$$\varphi_{a,b}(t) = t^{a-1}(1-t)^{b-1}/B(a,b) \quad \text{for } 0 \leq t \leq 1,$$

where $B(a,b)$ is the Beta-function and $a, b > 0$. The c.d.f. of $\beta_{a,b}$ is $\Pr\{\beta_{a,b} \leq t\} = I_t(a,b)$, where $I_t(a,b)$ is the regularised incomplete Beta-function, for which we use the convention

$$I_t(\cdot, \cdot) = \begin{cases} 0 & \text{for } t \leq 0 \\ 1 & \text{for } t \geq 1. \end{cases} \quad (5)$$

The following lemma (see, e.g., [2, Sect. 2.2]) will be used several times.

Lemma 2.1. *Let $X = (X_1, \dots, X_d) \stackrel{d}{=} R \cdot Z^{(d)}$ be a spherically symmetric random vector in \mathbb{R}^d . Then, for any $m \in \{1, \dots, d-1\}$, we have*

$$X^{(m)} = (X_1, \dots, X_m) \stackrel{d}{=} R \cdot \sqrt{\beta_{m/2, (d-m)/2}} \cdot Z^{(m)},$$

where $R = \|X\|$, $\beta_{m/2, (d-m)/2}$ and $Z^{(m)}$ are independent. Moreover, the joint density of $V^{(m)} = X^{(m)}/R$ is

$$\varphi_m(v_1, \dots, v_m) = \frac{\Gamma(d/2)}{\pi^{m/2} \Gamma((d-m)/2)} \left(1 - \sum_{i=1}^m v_i^2\right)^{(d-m)/2-1} \quad \text{for } \sum_{i=1}^m v_i^2 \leq 1.$$

The next proposition is the key element for the derivation of exact and asymptotic results on the behaviours of the mean distance c.d.f. and the (μ, s) -distortion.

Proposition 2.1. *Assume that $d \geq 2$ and $X \stackrel{d}{\sim} \mathbb{P}$ with \mathbb{P} spherically symmetric. Then, for any fixed $\mathbf{u} \in \mathbb{R}^d$ we have*

$$\|X - \mathbf{u}\|^2 \stackrel{d}{=} (\|\mathbf{u}\| - R)^2 + 4\|\mathbf{u}\| R \beta_{\delta, \delta}, \quad (6)$$

where $\delta = (d-1)/2$ and the random variables $R = \|X\|$ and $\beta_{\delta, \delta}$ are independent.

Moreover, when $\mathbf{R}_n \sim \mathbf{P} = \mathbb{P}_a^{[n]}$ with \mathbb{P}_a uniform on $\mathcal{S}_{d-1}(a)$, $a \geq 0$, we have

$$d^2(\mathbf{u}, \mathbf{R}_n) \stackrel{d}{=} (\|\mathbf{u}\| - a)^2 + 4a\|\mathbf{u}\| \zeta(n, d), \quad (7)$$

where $\zeta(n, d) = \min_{i=1, \dots, n} \zeta_i$ and the $\zeta_i \stackrel{d}{=} \beta_{\delta, \delta}$ are i.i.d.

Proof. As X is spherically symmetric, the distribution of $\|X - \mathbf{u}\|$ only depends on \mathbf{u} through $r = \|\mathbf{u}\|$, and without any loss of generality we can assume that $\mathbf{u} = (r, 0, \dots, 0)$. We thus have

$$\|X - \mathbf{u}\|^2 \stackrel{d}{=} (r - X_1)^2 + \sum_{j=2}^d X_j^2 = r^2 - 2rX_1 + R^2 = (R-r)^2 + 2rR(1 - Z_1),$$

where we have denoted $Z_1 = X_1/R$. From Lemma 2.1, R and Z_1 are independent and the expression of $\varphi_1(\cdot)$ gives $(1 - Z_1)/2 \stackrel{d}{=} \beta_{\delta, \delta}$, which yields (6). Since the n points of \mathbf{R}_n are i.i.d. with \mathbb{P}_a , the representation (6) yields (7). \square

From (6), for all $t \geq 0$ we have

$$\mathbb{P} \{\|X - \mathbf{u}\| \leq t\} = \Pr \{(R - r)^2 + 4Rr\beta_{\delta,\delta} \leq t^2\},$$

with $r = \|\mathbf{u}\| > 0$, and thus

$$\mathbb{P} \{\|X - \mathbf{u}\| \leq t\} = \Pr \left\{ \beta_{\delta,\delta} \leq \frac{t^2 - (R - r)^2}{4Rr} \right\}.$$

By conditioning on the random variable $R = \|X\|$ and denoting $\Phi(\cdot)$ the c.d.f. of $R = \|X\|$, we obtain

$$\begin{aligned} \mathbb{P} \{\|X - \mathbf{u}\| \leq t\} &= \int_{\rho \geq 0} \Pr \left\{ \beta_{\delta,\delta} \leq \frac{t^2 - (\rho - r)^2}{4\rho r} \right\} d\Phi(\rho) \\ &= \int_{\rho \geq 0} I_v(\delta, \delta) d\Phi(\rho), \end{aligned} \quad (8)$$

where

$$v = v(t, \rho, r) = [t^2 - (\rho - r)^2]/(4\rho r) \quad (9)$$

and $I_v(\cdot, \cdot)$ is the regularised incomplete beta-function with the added convention (5). The integration in (8) is over the support of the distribution of $R = \|X\|$. If $r = \|\mathbf{u}\| = 0$, then (8) reduces to

$$\mathbb{P} \{\|X - \mathbf{u}\| \leq t\} = \mathbb{P} \{\|X\| \leq t\} = \int_0^t d\Phi(\rho).$$

When $\mathbb{P} = \mathbb{P}_a$, the uniform distribution on the sphere $\mathcal{S}_{d-1}(a)$, the expression (8) with the convention (5) can be simplified as follows:

$$\mathbb{P}_a \{\|X - \mathbf{u}\| \leq t\} = \begin{cases} 0 & \text{if } t \leq |r - a|, \\ I_v(\delta, \delta) & \text{if } |r - a| \leq t \leq a + r, \\ 1 & \text{if } a + r \leq t, \end{cases} \quad (10)$$

where $r = \|\mathbf{u}\|$ and $v = v(t, a, r)$ is given by (9).

2.4 $F_n(t; \mathbb{P}^{[n]}, \mu)$ and $D_{\mu,s}(\mathbb{P}^{[n]})$ when \mathbb{P} is spherically symmetric

From (3) and (4), the mean distance c.d.f. $F_n(\cdot; \mathbb{P}^{[n]}, \mu)$ can be calculated explicitly as

$$F_n(t; \mathbb{P}^{[n]}, \mu) = 1 - \mathbb{E}_\mu \left\{ \left(1 - \mathbb{P} \{\|X - U\| \leq t\} \right)^n \right\}, \quad (11)$$

where $U \stackrel{d}{\sim} \mu$, $X \stackrel{d}{\sim} \mathbb{P}$, and X and U are independent. When \mathbb{P} is spherically symmetric, $\mathbb{P} \{\|X - \mathbf{u}\| \leq t\}$ is given by (8) which only depends on \mathbf{u} through $r = \|\mathbf{u}\|$, and the expectation with respect to U in (11) is reduced to an expectation with respect to the distribution of $\|U\|$. The calculation of $F_n(t; \mathbb{P}^{[n]}, \mu)$ thus amounts to a double integration, with respect to the distributions of $\|X\|$ and $\|U\|$. From (2), the calculation of $D_{\mu,s}(\mathbb{P}^{[n]})$ requires an additional integration with respect to t ,

$$\begin{aligned} D_{\mu,s}(\mathbb{P}^{[n]}) &= s \int_{t \geq 0} t^{s-1} \mathbb{E}_\mu \left\{ \left(1 - \mathbb{P} \{\|X - U\| \leq t\} \right)^n \right\} dt, \\ &= s \int_{t \geq 0} t^{s-1} \int_{r \geq 0} H(r, t; \Phi, n) d\Psi(r) dt, \end{aligned} \quad (12)$$

where

$$H(r, t; \Phi, n) = \left(1 - \int_{\rho \geq 0} I_v(\delta, \delta) d\Phi(\rho) \right)^n,$$

with $v = v(t, \rho, r)$ given by (9), $\Psi(\cdot)$ the c.d.f. of $\|U\|$ for $U \stackrel{d}{\sim} \mu$ and $\Phi(\cdot)$ the c.d.f. of $\|X\|$ for $X \stackrel{d}{\sim} \mathbb{P}$.

The integrals required to compute $D_{\mu, s}(\mathbb{P}^{[n]})$ can be evaluated with arbitrary precision. When \mathbb{P} is appropriately parameterised, a high-performance random quantiser can be obtained by numerically minimising the distortion with respect to its defining parameters. For the remainder of this paper, we focus on quantisers defined by a distribution \mathbb{P} that depends on a single scalar parameter: the radius of a sphere (Section 3.1), the radius of a ball (Section 3.3), or the variance of a multivariate normal distribution (Section 3.4). The optimisation is performed using a derivative-free line-search method, specifically the golden-section algorithm.

Remark 2.2. *The expression (12) gives the expected (μ, s) -distortion for random quantisers. Therefore, according to the paradigm of the so-called “probabilistic method” (see, e.g., [1]), for any \mathbb{P} there exists at least one non-random n -point set \mathbf{X}_n with (μ, s) -distortion $E_{\mu, s}^s(\mathbf{X}_n) \leq D_{\mu, s}(\mathbb{P}^{[n]})$. See Section 3.2 for an illustration involving full factorial designs. \triangleleft*

3 Exact, non-asymptotic, results

Throughout this section, three emblematic cases of spherically symmetric measures are investigated. Nevertheless, the results remain valid for any measure ν , regardless of its symmetry, so long as the radial component $r = \|U\|$ follows the same distribution under ν as under μ . For instance, in Section 3.1 (μ uniform on $\mathcal{S}_{d-1}(1)$), ν can be a point mass $\delta_{\mathbf{u}}$ for any unit vector \mathbf{u} ; in Sections 3.3 (μ uniform in $\mathcal{B}_d(1)$) and 3.4 (μ normal), ν may be supported on a line segment or a line, respectively, provided the distribution of r is preserved.

3.1 μ is uniform on the unit sphere $\mathcal{S}_{d-1}(1)$

Here μ is the spherical measure (uniform on $\mathcal{S}_{d-1}(1)$), and the distribution of $\|U\|$ for $U \stackrel{d}{\sim} \mu$ is the delta measure at $r = 1$. When $n = 1$ and $\mathbf{X}_n = \{\mathbf{0}_d\}$, the distance c.d.f. $F(t; \mathbf{X}_n, \mu)$ equals 0 for $t < 1$ and 1 for $t \geq 1$. For any other \mathbf{X}_n it has a density $f(\cdot; \mathbf{X}_n, \mu)$ on $[0, \text{CR}(\mathbf{X}_n)]$.

We first consider random quantisers with distribution $\mathbb{P} = \mathbb{P}_a$ uniform on $\mathcal{S}_{d-1}(a)$ and minimise $D_{\mu, s}(\mathbb{P}_a^{[n]})$ with respect to $a \in [0, 1]$. The expression (10) can be simplified as follows:

$$\mathbb{P}_a \{ \|X - \mathbf{u}\| \leq t \} = \begin{cases} 0 & \text{if } t \leq 1 - a, \\ I_v(\delta, \delta) & \text{if } 1 - a \leq t \leq 1 + a, \\ 1 & \text{if } 1 + a \leq t, \end{cases}$$

where $v = [t^2 - (1 - a)^2]/(4a)$. Formula (12) then gives

$$D_{\mu, s}(\mathbb{P}_a^{[n]}) = (1 - a)^s + s \int_{1-a}^{1+a} t^{s-1} [1 - I_v(\delta, \delta)]^n dt. \quad (13)$$

This exact expression for the expected (μ, s) -distortion depends on d, n, s and a ; the value $a^* = a^*(d, n, s)$ that minimises $D_{\mu, s}(\mathbb{P}_a^{[n]})$ with respect to a can be obtained numerically with arbitrary precision for any given d, n and s . In the special case

$d = 3$, $\delta = 1$ and $I_v(1, 1) = v$ for $v \in [0, 1]$, so that $D_{\mu, s}(\mathbb{P}_a^{[n]})$ can be calculated explicitly for s even. It is given by a polynomial in a of degree s , with for example $D_{\mu, 2}(\mathbb{P}_a^{[n]}) = (1 - a)^2 + 4a/(n + 1)$ and $D_{\mu, 4}(\mathbb{P}_a^{[n]}) = (1 - a)^4 + 8a[n(1 - a)^2 + 2 + 2a^2]/[(n + 1)(n + 2)]$, which gives $a^*(3, n, 2) = (n - 1)/(n + 1)$ and $a^*(3, n, 4)$ as the root of a cubic equation, which satisfies $a^*(3, n, 4) = 1 - 4/n + 16/n^2 + \mathcal{O}(1/n^3)$ as $n \rightarrow \infty$.

The left column of Figure 1 presents $a^*(d, n, s)$ as a function of d for different n and $s = 1$ (top) and $s = 10$ (bottom). For fixed s and d , a^* increases with n , and asymptotically, when n tends to infinity, a^* tends to 1 (see, e.g., [4, Chap. 9]). Intuitively the choice $a = 1$ seems natural for all n and s . However, Figure 1 indicates that $a = 1$ can be a poor choice, especially in high dimension. For any fixed d and n , $a^*(d, n, s) \rightarrow 1$ when $s \rightarrow 0$ and is a decreasing function of s , with $a^*(d, n, \infty) = 0$ if n is small enough. Indeed, for $n \leq d$, $\text{CR}(\mathbf{X}_n) \geq 1$ for any \mathbf{X}_n and the inequality is strict if $\mathbf{0}_n \notin \mathbf{X}_n$. This follows from the fact that any d points in \mathbb{R}^d belong to a d -dimensional hyperplane \mathcal{H}_d ; one of the two parts of $\mathcal{S}_{d-1}(1)$ cut by \mathcal{H}_d necessarily contains a hemisphere whose pole is at distance at least one from each point. This implies that $a^*(d, n, s) = 0$ for large enough s when $n \leq d$. Also, for fixed n and s , $a^*(d, n, s)$ decreases with d .

The central column of Figure 1 shows that, as expected, $D_{\mu, s}^{1/s}(\mathbb{P}_{a^*}^{[n]})$ decreases with n and increases with d and s . The right column presents the efficiency of the naive quantiser with n points i.i.d. on $\mathcal{S}_{d-1}(1)$ relative to optimised random quantisers with n points on $\mathcal{S}_{d-1}(a^*)$. It shows that the benefit of using an appropriate a is significant when d is large or n is small.

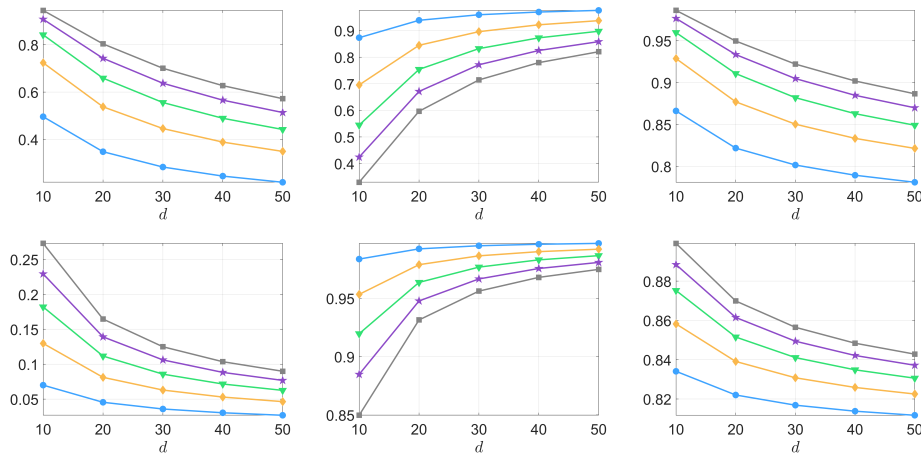


Figure 1: Sphere. Value a^* minimising $D_{\mu, s}(\mathbb{P}_a^{[n]})$ (left column), $D_{\mu, s}^{1/s}(\mathbb{P}_{a^*}^{[n]})$ (central column) and ratio $D_{\mu, s}^{1/s}(\mathbb{P}_{a^*}^{[n]})/D_{\mu, s}^{1/s}(\mathbb{P}_1^{[n]})$ (right column) as functions of d for $s = 1$ (top row) and $s = 10$ (bottom row) and different values of n : $n = 10$ (\bullet), $n = 10^2$ (\blacklozenge), $n = 10^3$ (\blacktriangledown), $n = 10^4$ (\blackstar), and $n = 10^5$ (\blacksquare).

The next figure (Figure 2, where $s = 10$, $d = 10$) shows that adding a delta measure at $\mathbf{0}_d$ to \mathbb{P}_1 may also yield a decrease of the expected distortion for small n . Denote $\mathbb{Q}_{\alpha, a} = \alpha \mathbb{P}_a + (1 - \alpha) \delta_{\mathbf{0}_d}$. Similarly to (13), we obtain

$$D_{\mu, s}(\mathbb{Q}_{\alpha, a}^{[n]}) = (1 - a)^s + s \int_{1-a}^1 t^{s-1} [1 - \alpha I_v(\delta, \delta)]^n dt + s \alpha^n \int_1^{1+a} t^{s-1} [1 - I_v(\delta, \delta)]^n dt,$$

with $v = [t^2 - (1 - a)^2]/(4a)$. The left panel presents the optimal α^* minimising $D_{\mu,s}(\mathbb{Q}_{\alpha^*,1}^{[n]})$ as a function of n : unsurprisingly, α^* quickly approaches 1 as n increases. One may observe that, for all n , $(1 - \alpha^*) > 1/n$ (it corresponds to the probability that a realisation of a random set \mathbf{R}_n contains a point at $\mathbf{0}_d$). Next, for a given n ($n = 20$), we use the corresponding optimal α^* minimising $D_{\mu,s}(\mathbb{Q}_{\alpha^*,1}^{[n]})$ ($\alpha^* \simeq 0.846$) and plot $D_{\mu,s}^{1/s}(\mathbb{Q}_{\alpha^*,a}^{[n]})$ and $D_{\mu,s}^{1/s}(\mathbb{Q}_{1,a}^{[n]}) = D_{\mu,s}^{1/s}(\mathbb{P}_a^{[n]})$ as functions of a (central panel): the effect of introducing a delta measure at $\mathbf{0}_d$ is significant for a close to one, but choosing a suitable radius a has bigger impact. Finally, we consider the efficiencies of random quantisers with $\mathbb{Q}_{\alpha^*,1}$ with respect to quantisers distributed with \mathbb{P}_1 and \mathbb{P}_{a^*} (with α^* and a^* depending on n) as functions of n (right panel): when a is set to 1, the choice of a suitable α has some positive effect for small n , but the impact of choosing a suitable a is stronger for all n .

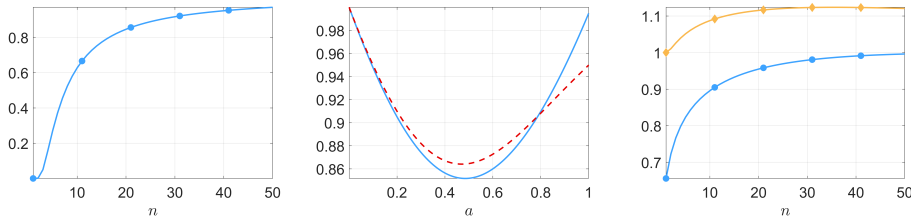


Figure 2: Left: value α^* minimising $D_{\mu,s}(\mathbb{Q}_{\alpha^*,1}^{[n]})$ as function of n . Center: $D_{\mu,s}^{1/s}(\mathbb{Q}_{\alpha^*,a}^{[n]})$ (---) and $D_{\mu,s}^{1/s}(\mathbb{Q}_{1,a}^{[n]})$ (—) as functions of a for $n = 20$ and $\alpha^* = 0.846$. Right: $D_{\mu,s}^{1/s}(\mathbb{Q}_{\alpha^*,1}^{[n]})/D_{\mu,s}^{1/s}(\mathbb{P}_1^{[n]})$ (●) and $D_{\mu,s}^{1/s}(\mathbb{Q}_{\alpha^*,1}^{[n]})/D_{\mu,s}^{1/s}(\mathbb{P}_{a^*}^{[n]})$ (◆) as functions of n ; $s = 10$, $d = 10$.

3.2 Comparison between random quantisers uniform on a sphere and optimised full factorial 2^d designs

Let $n = 2^d$ and $\mathbf{X}_n(b)$ be the full factorial 2^d design with points \mathbf{x}_i having coordinates $\pm b$, $b \in (0, 1]$: the \mathbf{x}_i are vertices of the cube $[-b, b]^d$; they also belong to the sphere $\mathcal{S}_{d-1}(a)$ with $a = \sqrt{d}b$. For $\mathcal{X} = \mathcal{S}_{d-1}(1)$, the Voronoi regions $\mathcal{V}(\mathbf{x}_i) = \{\mathbf{x} \in \mathcal{X} : \|\mathbf{x} - \mathbf{x}_i\| = \min_{\mathbf{x}_j \in \mathbf{X}_n(b)} \|\mathbf{x} - \mathbf{x}_j\|\}$ are all identical up to a permutation of coordinates and do not depend on the value of b .

Consider first the case $s = 2$. For μ uniform on $\mathcal{X} = \mathcal{S}_{d-1}(1)$, $E_{2,\mu}^2[\mathbf{X}_n(b)] = \mathbb{E}\{\|V - \mathbf{b}\|^2\}$ where $\mathbf{b} = (b, \dots, b) \in \mathbb{R}^d$ and $V = (V_1, \dots, V_d)$ is uniform in $\mathcal{V}(\mathbf{b}) = \mathcal{S}_{d-1}(1) \cap \mathbb{R}_+^d$. Therefore

$$E_{2,\mu}^2[\mathbf{X}_n(b)] = \mathbb{E}\{\|V\|^2 - 2b \sum_{i=1}^d V_i + db^2\} = 1 - 2bd \mathbb{E}\{V_1\} + db^2.$$

Minimisation of $E_{2,\mu}^2[\mathbf{X}_n(b)]$ with respect to b yields $b_2^* = \mathbb{E}\{V_1\}$ and the optimal $(\mu, 2)$ -distortion of a 2^d factorial design is $E_{2,\mu}^2[\mathbf{X}_n(b_2^*)] = 1 - d(b_2^*)^2$. For $U^{(d)} = (U_1, \dots, U_d) \stackrel{d}{\sim} \mu$, the first component U_1 has the density $\varphi_1(\cdot)$ of Lemma 2.1 on $[-1, 1]$, therefore, V_1 has the density $2\varphi_1(\cdot)$ on $[0, 1]$, so that

$$\begin{aligned} b_2^* = \mathbb{E}\{V_1\} &= \frac{\Gamma(d/2)}{\sqrt{\pi} \Gamma((d+1)/2)}, \\ E_{2,\mu}^2[\mathbf{X}_n(b_2^*)] &= 1 - \frac{d}{\pi} \left(\frac{\Gamma(d/2)}{\Gamma((d+1)/2)} \right)^2. \end{aligned}$$

More generally, the analytic expression for the (μ, s) -distortion $E_{\mu, s}^s[\mathbf{X}_n(b)]$ can be derived for any even s , but the calculations become more complicated as s increases. For $s = 4$ we obtain

$$\begin{aligned} E_{4, \mu}^4[\mathbf{X}_n(b)] &= \mathbf{E}\{\|V - \mathbf{b}\|^4\} \\ &= 1 + 4b^2 \mathbf{E}\left\{\left(\sum_{i=1}^d V_i\right)^2\right\} + d^2b^4 + 2db^2 - 4bd \mathbf{E}\{V_1\}(1 + db^2). \end{aligned}$$

Using $\mathbf{E}\{(\sum_{i=1}^d V_i)^2\} = 1 + d(d-1)\mathbf{E}\{V_1V_2\}$, where $\mathbf{E}\{V_1V_2\} = 2/(\pi d)$ from $\varphi_2(\cdot, \cdot)$ of Lemma 2.1, together with the expression above for $\mathbf{E}\{V_1\}$, we can express $E_{4, \mu}^4[\mathbf{X}_n(b)]$ as a fourth-degree polynomial in b with coefficients depending on d . The optimal value b_4^* can be obtained explicitly. The values of b_2^* and b_4^* are very close for large d as $a_j^* = \sqrt{d}b_j^* = \sqrt{2/\pi} + \mathcal{O}(1/d)$ for $j = 2, 4$.

For $s = \infty$, $E_{\infty, \mu}[\mathbf{X}_n(b_\infty^*)] = \text{CR}[\mathbf{X}_n(b)]$, the covering radius of $\mathbf{X}_n(b)$, with $(\text{CR}[\mathbf{X}_n(b)])^2 = 1 + db^2 - 2b$ being minimum for $b_\infty^* = 1/d$, which gives $\text{CR}[\mathbf{X}_n(b_\infty^*)] = \sqrt{1 - 1/d}$.

Figure 3 compares the optimal full factorial designs $\mathbf{X}_n(b_s^*)$ for $s = 2$ and 4 with optimised random quantisers $\mathbb{P}_{a_s^*}^{[n]}$ on $\mathcal{S}_{d-1}(1)$ with the same sample size $n = 2^d$. The left panel shows the values of the radii of the various spheres on which the points lie, as functions of d . The right panel presents $D_{\mu, s}^{1/s}(\mathbb{P}_{a_s^*}^{[n]})$ for the random quantisers and $E_{\mu, s}[\mathbf{X}_n(b_s^*)]$ for the full factorial designs, for $s = 2$ and 4. For both types of point sets, the behaviours for $s = 2$ and $s = 4$ are similar. As d tends to infinity, for the full factorial designs $a_s^* = \sqrt{d}b_s^*$ tends to the limit $\sqrt{2/\pi} \simeq 0.797885$ from above. For random quantisers, we observe that $a^*(s) = a^*(d, n, s)$ defined in Section 3.1 tends from below to a larger limiting value—we shall see in Section 4.3 that this limiting value equals $\sqrt{3}/2 \simeq 0.8660$. The expected (μ, s) -distortion of random quantisers shows little sensitivity to the choice of a in the neighborhood of $a^*(s)$. In particular, the plots of $D_{\mu, s}^{1/s}(\mathbb{P}_{a_s^*}^{[n]})$ (not shown) and $D_{\mu, s}^{1/s}(\mathbb{P}_{a^*(s)}^{[n]})$ almost coincide for $d > 3$.

For both values of s , $a_s^* \approx a^*(s)$ for $d = 7$. This dimension is the critical one at which random quantisers start exhibiting a smaller quantisation error than full factorial designs. As a consequence of the probabilistic method, it implies that for all $d \geq 7$ there exist non-random quantisers with $n = 2^d$ that have smaller quantisation errors for $s = 2$ and 4 than optimised full factorial designs.

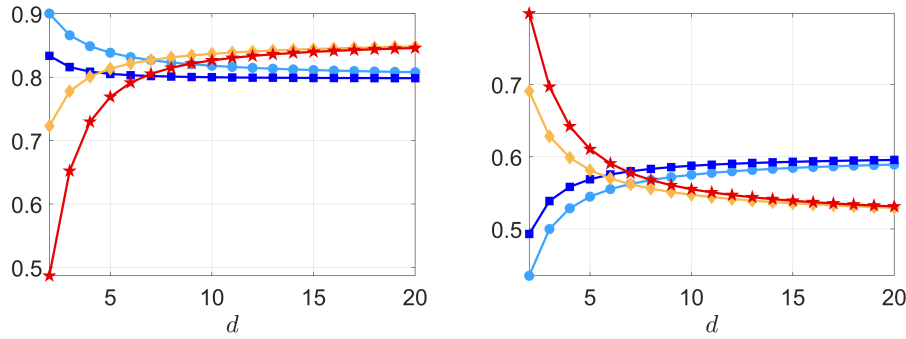


Figure 3: Left: Values $a^*(s)$ minimising $D_{\mu, s}(\mathbb{P}_{a^*}^{[n]})$ for $n = 2^d$ with $s = 2$ (\diamond) and $s = 4$ (\star), and values $a_s^* = \sqrt{d}b_s^*$ minimising $E_{\mu, s}[\mathbf{X}_n(b)]$ for $s = 2$ (\bullet) and $s = 4$ (\blacksquare), as functions of d . Right: $D_{\mu, s}^{1/s}(\mathbb{P}_{a^*}^{[n]})$ for $n = 2^d$ with $a^* = a^*(d, n, s)$, $s = 2$ (\diamond) and $s = 4$ (\star), and values $E_{\mu, s}[\mathbf{X}_n(b_s^*)]$ for $s = 2$ (\bullet) and $s = 4$ (\blacksquare), as functions of d .

3.3 μ is uniform in the unit ball $\mathcal{B}_d(1)$

For μ uniform in $\mathcal{B}_d(1)$, the density of $r = \|U\|$ for $U \stackrel{d}{\sim} \mu$ is $\psi(\tau) = d\tau^{d-1}$.

Consider first the case where $\mathbb{P} = \mathbb{P}_a$ uniform on $\mathcal{S}_{d-1}(a)$: (12) gives

$$D_{\mu,s}(\mathbb{P}_a^{[n]}) = s \int_{t \geq 0} t^{s-1} \int_{r \geq 0} H(r, t; \Phi_a, n) \psi(r) dr dt, \quad (14)$$

where $H(r, t; \Phi_a, n) = \left(1 - \mathbb{P}_a\{\|X - \mathbf{u}\| \leq t\}\right)^n$ with $\Phi_a(\cdot)$ the c.d.f. of the delta measure δ_a and $r = \|\mathbf{u}\|$, so that $\mathbb{P}_a\{\|X - \mathbf{u}\| \leq t\}$ is given by (10).

We also consider random quantisers whose n points are i.i.d. with $\mathbb{P} = \mathbb{P}_{0,b}$ uniform in $\mathcal{B}_d(b)$. The c.d.f. $\Phi(\cdot)$ of $R = \|X\|$ has then the density $\phi_{0,b}(\rho) = d\rho^{d-1}/b^d$ for $\rho \in [0, b]$. More general spherically symmetric distributions \mathbb{P} could also be used, but we found that, unless n is extremely small, the class of distributions $\mathbb{P}_{0,b}$ is rich enough. The expected (μ, s) -distortion $D_{\mu,s}(\mathbb{P}_{0,b}^{[n]})$ is given by (12) where

$$H(r, t; \Phi, n) = \left(1 - \int_a^b I_v(\delta, \delta) \phi_{0,b}(\rho) d\rho\right)^n,$$

with $v = v(t, \rho, r)$ given by (9).

Figure 4 presents the same information as Figure 1 for the ball configuration: we consider optimal design defined by \mathbb{P}_{0,b^*} , where $b^* = b^*(d, n, s)$ minimises $D_{\mu,s}(\mathbb{P}_{0,b}^{[n]})$ and the right column compares performances of \mathbb{P}_{0,b^*} and $\mathbb{P}_{0,1}$.

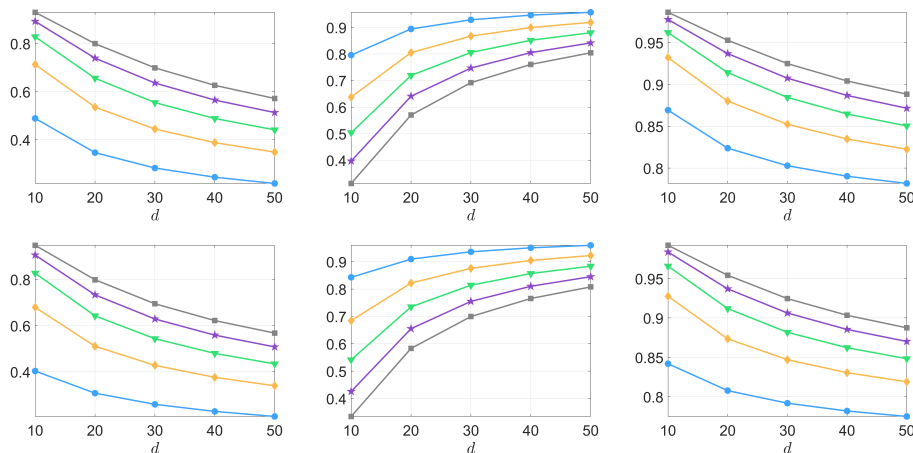


Figure 4: Ball. Value b^* minimising $D_{\mu,s}(\mathbb{P}_{0,b}^{[n]})$ (left column), $D_{\mu,s}^{1/s}(\mathbb{P}_{0,b^*}^{[n]})$ (central column) and ratio $D_{\mu,s}^{1/s}(\mathbb{P}_{0,b^*}^{[n]})/D_{\mu,s}^{1/s}(\mathbb{P}_{0,1}^{[n]})$ (right column) as functions of d for $s = 1$ (top row) and $s = 10$ (bottom row) and different values of n : $n = 10$ (\bullet), $n = 10^2$ (\blacklozenge), $n = 10^3$ (\blacktriangledown), $n = 10^4$ (\blackstar), and $n = 10^5$ (\blacksquare).

The quantities considered behave qualitatively as in Figure 1. Note, however, that b^* is larger than a^* plotted in Figure 1 (left columns— b^* is much larger than a^* on the bottom row with $s = 10$), that $D_{\mu,s}(\mathbb{P}_{0,b^*}^{[n]})$ is smaller than $D_{\mu,s}(\mathbb{P}_{0,a^*}^{[n]})$ (central columns), and that the efficiency of a “classical” random design compared to an optimised design is slightly larger for the ball than for the sphere (right columns). For a fixed dimension d , the empirical distribution of an optimal quantiser which minimises $E_{\mu,s}(\mathbf{X}_n)$ converges weakly to $\mathbb{P}_{0,1}^{[n]}$ as $n \rightarrow \infty$ (see [4, Table 7.1]). Consistent with this theoretical result, we empirically observe that the optimal

parameters b^* and a^* both converge to 1 as $n \rightarrow \infty$; see also Section 4.4.1 for further details on their asymptotic behaviour.

Figure 12 of Section 4.4.1 displays the optimal values $b^*(d, n, s)$ and $a^*(d, n, s)$, respectively minimising $D_{\mu, s}(\mathbb{P}_{0, b}^{[n]})$ and $D_{\mu, s}(\mathbb{P}_{a}^{[n]})$, plotted as functions of d for $s = 2$ and two distinct values of n . The figure shows that $b^* > a^*$, and the gap $b^* - a^*$ narrows as d increases, reflecting the fact that both a^* and b^* converge to zero as $d \rightarrow \infty$. The behaviour remains qualitatively unchanged for other values of s , especially when the dimension d is large.

Given the observations in Figures 4 and 12, two key patterns emerge: (i) for large dimensions d , the values of $a^*(d, n, s)$ and $b^*(d, n, s)$ become very close; (ii) the quantiser $\mathbb{P}_{0, b^*}^{[n]}$ significantly outperforms $\mathbb{P}_{0, 1}^{[n]}$ when d is sufficiently large. Moreover, we also observe that $\mathbb{P}_{a^*}^{[n]}$ outperforms $\mathbb{P}_{0, b^*}^{[n]}$ for reasonable design sizes n ; see Figure 13 in Section 4.4.1. Since b^* converges to 1 as $n \rightarrow \infty$, with $\mathbb{P}_{0, 1}^{[n]}$ being asymptotically optimal, a natural question arises: for a fixed dimension d , at what sample size $n = n^*(d, s)$ does $\mathbb{P}_{a^*}^{[n]}$ stop being preferable to $\mathbb{P}_{0, b^*}^{[n]}$? Empirical analysis reveals that this transition occurs only for extremely large values of n . Define

$$n^*(d, s) = \max\{n \in \mathbb{N} : D_{\mu, s}(\mathbb{P}_{a^*}^{[n]}) < D_{\mu, s}(\mathbb{P}_{0, b^*}^{[n]})\}. \quad (15)$$

The left panel of Figure 5 presents $n^*(d, s)$ (in log scale, obtained by dichotomous search) as a function of $d = 3, \dots, 20$ for three values of s , indicating a superexponential increase of $n^*(d, s)$ with d .

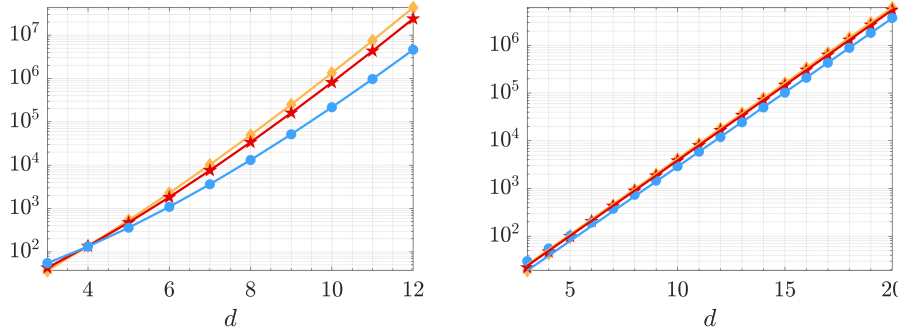


Figure 5: $n^*(d, s)$ as a function of d for $s = 2$ (\diamond), $s = 4$ (\star) and $s = 10$ (\bullet). Left: μ is uniform on $\mathcal{S}_{d-1}(1)$ and $n^*(d, s)$ is given by (15). Right: μ is spherically normal and $n^*(d, s)$ is given by (17).

3.4 μ is a spherically symmetric normal distribution

Any spherically symmetric normal distribution in \mathbb{R}^d can be renormalised as $\mathcal{N}(\mathbf{0}_d, \mathbf{I}_d/d)$, with \mathbf{I}_d the d -dimensional identity matrix. In this section, we assume that μ is the corresponding probability measure. When $U \stackrel{d}{\sim} \mu$, $d\|U\|^2$ has the chi-square distribution with d degrees of freedom, so that the density of $\|U\|$ is

$$\psi(r) = \frac{d^{d/2}}{2^{d/2-1} \Gamma(d/2)} r^{d-1} e^{-dr^2/2}, \quad r \geq 0. \quad (16)$$

The distribution of r is more and more concentrated around 1 as d increases. Its k -th moment is

$$M_{\psi, k} = \mathbf{E}_{\mu}\{\|U\|^k\} = (2^{k/2}/d^{k/2})\Gamma((k+d)/2)/\Gamma(d/2), \quad k = 1, 2, \dots$$

so that its mean is smaller than 1 for any d and its variance is $1/(2d) - 1/(8d^2) + \mathcal{O}(1/d^3)$, $d \rightarrow \infty$.

When $\mathbb{P} = \mathbb{P}_a$ uniform on $\mathcal{S}_{d-1}(a)$, the expected (μ, s) -distortion $D_{\mu,s}(\mathbb{P}_a^{[n]})$ is given by (14), with $\psi(\cdot)$ given by (16).

When $\mathbb{P} = \mu_\sigma$ is the probability measure of $\mathcal{N}(\mathbf{0}_d, \sigma^2 \mathbf{I}_d/d)$, $R = \|X\|$ has the p.d.f. $\phi_\sigma(\rho) = (1/\sigma)\psi(\rho/\sigma)$ where $\psi(\cdot)$ given by (16), and the expected (μ, s) -distortion $D_{\mu,s}(\mu_\sigma^{[n]})$ is given by (12) where

$$H(r, t; \Phi, n) = \left(1 - \frac{1}{\sigma} \int_{\rho \geq 0} I_v(\delta, \delta) \psi(\rho/\sigma) d\rho\right)^n,$$

with $v = v(t, \rho, r)$ given by (9).

Let $\sigma^* = \sigma^*(d, n, s)$ denote the value of σ that minimises the distortion $D_{\mu,s}(\mu_\sigma^{[n]})$ and $a^* = a^*(d, n, s)$ denote the value of a that minimises $D_{\mu,s}(\mathbb{P}_a^{[n]})$, as in previous sections.

The empirical distribution of an optimal quantiser \mathbf{X}_n^* minimising $E_{\mu,s}(\mathbf{X}_n)$ weakly converges to $\mathcal{N}(\mathbf{0}_d, \sigma_\infty^* \mathbf{I}_d/d)$ as $n \rightarrow \infty$, with $\sigma_\infty^* = 1 + s/d$; see [4, Table 7.1]. Figure 6 illustrates that $\sigma^* = \sigma^*(d, n, s)$ increases with s , similarly to σ_∞^* , and that $a^* = a^*(d, n, s)$ also increases with s , contrary to Sections 3.1 and 3.3. The reason is that large values of $r = \|U\|$ get increasing importance as s increases, while $r = 1$ in Section 3.1 and $r \leq 1$ in Section 3.3. Note that $\sigma^*(d, n, s)$ is significantly smaller than $\sigma_\infty^* = 1 + s/d$ (Figure 6 is for $d = 10$).

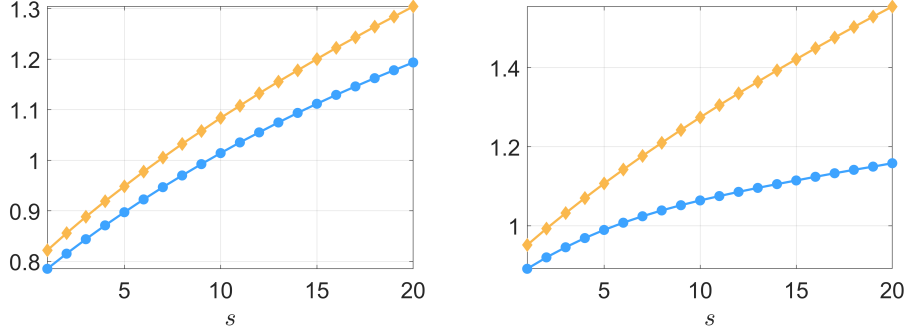


Figure 6: Optimal values $a^*(d, n, s)$ (●) and $\sigma^*(d, n, s)$ (◆) as functions of s for $d = 10$, $n = 1000$ (left) and $n = 100000$ (right).

Figure 7 presents $D_{\mu,s}^{1/s}(\mu_\sigma^{[n]})$ and $D_{\mu,s}^{1/s}(\mathbb{P}_{a=\sigma}^{[n]})$ as functions of σ for $s = 2$, $n = 1000$ and $d = 5, 10$ and 20 . Note that, already for $d = 5$ (left panel), 1 000 points are not enough for $\sigma^* = \sigma^*(d, n, s) \simeq 1.1832$ to approach the asymptotically optimal value $\sigma_\infty^* = 1.4$. For $d \geq 10$ (center and right panels) the plots of $D_{\mu,s}^{1/s}(\mathbb{P}_\sigma^{[n]})$ and $D_{\mu,s}^{1/s}(\mu_\sigma^{[n]})$ are close, especially near their minima. The behaviour is similar when using other values of s .

The left panel of Figure 8 shows that $\sigma^* - a^*$ tends to zero as d increases, a consequence of $D_{\mu,s}(\mu_\sigma^{[n]})$ tending to $D_{\mu,s}(\mathbb{P}_\sigma^{[n]})$. Moreover, as d grows, $\psi(\cdot)$ is more and more concentrated around 1. This explains why for $d \geq 10$ the values of a^* are close to those obtained for μ uniform on $\mathcal{S}_{d-1}(1)$; see the curves on Figure 1-top-left (they are plotted for $s = 1$ but those obtained for $s = 2$ are very similar). The right panel presents the efficiencies of the asymptotically optimal distribution $\mu_{\sigma_\infty^*}$ relative to \mathbb{P}_{a^*} and μ_{σ^*} , for $n = 10000$, as functions of d . These efficiencies

are always less than 1, meaning that the asymptotic regime is not yet reached for the values of d considered. At $d = 10$, however, we can observe that, contrary to the central panel of Figure 7 where $n = 1000$, now $D_{\mu,2}(\mathbb{P}_{a^*}^{[n]}) > D_{\mu,2}(\mu_{\sigma^*}^{[n]})$: with $n = 10000$ points we approach the asymptotic regime and \mathbb{P}_{a^*} is dominated by a suitably chosen normal distribution.

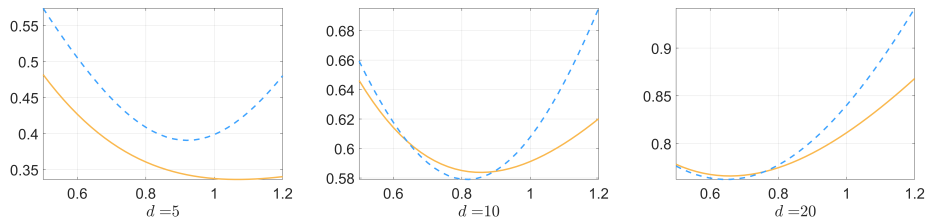


Figure 7: $D_{\mu,s}^{1/s}(\mathbb{P}_{a^*}^{[n]})$ (---) and $D_{\mu,s}^{1/s}(\mu_{\sigma^*}^{[n]})$ (—) as functions of σ for different d with $n = 1000$ and $s = 2$.

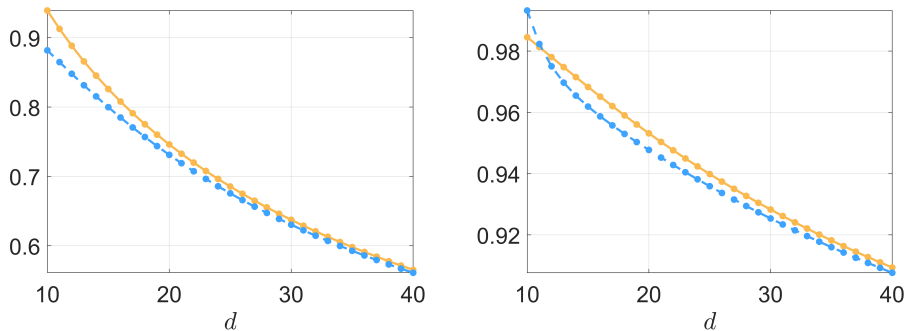


Figure 8: Left: Optimal values $a^*(d, n, s)$ (---) and $\sigma^*(d, n, s)$ (—) as functions of d . Right: ratios $D_{\mu,s}^{1/s}(\mathbb{P}_{a^*}^{[n]})/D_{\mu,s}^{1/s}(\mu_{\sigma^*}^{[n]})$ (---) and $D_{\mu,s}^{1/s}(\mu_{\sigma^*}^{[n]})/D_{\mu,s}^{1/s}(\mu_{\sigma_\infty}^{[n]})$ (—) as functions of d for $s = 2$ and $n = 10000$.

In view of the right panel of Figure 8, and following the analysis in Section 3.3, we investigate the following question: for a fixed dimension d , up to which sample size n does the random quantiser $\mathbb{P}_{a^*}^{[n]}$ outperform $\mu_{\sigma^*}^{[n]}$? Defining

$$n^*(d, s) = \max\{n \in \mathbb{N} : D_{\mu,s}(\mathbb{P}_{a^*}^{[n]}) < D_{\mu,s}(\mu_{\sigma^*}^{[n]})\}, \quad (17)$$

in the right panel of Figure 5 we present $n^*(d, s)$ (in log scale) as a function of $d = 3, \dots, 20$ for three values of s . The straight lines fitted to these logarithmic plots show almost perfect coincidence between $n^*(d, s)$ and the exponential increase $n_0 \lambda^d$, with numerical values of n_0 and λ depending weakly on s : $n_0 \simeq 2.81, 2.68, 2.21$ and $\lambda \simeq 2.08, 2.07, 2.05$ for $s = 2, 4$ and 10 , respectively.

4 Extreme-value approximations

In this section, extreme-value theory is used to derive approximations of the (μ, s) -distortion $D_{\mu,s}(\mathbb{P}_a^{[n]})$, where \mathbb{P}_a is uniform on $\mathcal{S}_{d-1}(a)$ (Section 4.1). In Section 4.2, three asymptotic regimes are identified that govern the limiting behaviour of $D_{\mu,s}(\mathbb{P}_a^{[n]})$ when n increases with d . The case where μ is uniform on $\mathcal{S}_{d-1}(1)$ is considered

first (Section 4.3): we show that to each asymptotic regime is associated a limiting value of the optimal radius a^* that does not depend on s . In Section 4.4, these results are extended to general spherically symmetric measures μ satisfying a norm-concentration property, with the uniform distribution in $\mathcal{B}_d(1)$ and the multivariate normal distribution as illustrative examples.

4.1 Uniform quantisers on a sphere

Consider random quantisers \mathbf{R}_n with distribution $\mathbf{P} = \mathbb{P}_a^{[n]}$ where \mathbb{P}_a is uniform on $\mathcal{S}_{d-1}(a)$. For large n , the distribution of $\zeta(n, d)$ in (7) can be approximated using standard results from extreme-value theory. Here we assume $d \geq 3$ to avoid singularity in beta distributions.

Lemma 4.1. *Assume that $d \geq 3$ and $\mathbf{P} = \mathbb{P}_a^{[n]}$. For any fixed $\mathbf{u} \in \mathbb{R}^d$, we have*

$$\frac{1}{4a \|\mathbf{u}\| \kappa_{n,d}} [d^2(\mathbf{u}, \mathbf{R}_n) - (\|\mathbf{u}\| - a)^2] \stackrel{d}{\rightarrow} \xi_d, \quad n \rightarrow \infty, \quad (18)$$

where ξ_d is a random variable with Weibull c.d.f. $F_d(t) = 1 - \exp(-t^\delta)$, $t \geq 0$, and moments $\mathbb{E}\{\zeta_d^k\} = \Gamma(1 + k/\delta)$ with $\delta = (d-1)/2$, and where $\kappa_{n,d}$ is the $1/n$ quantile of $\beta_{\delta,\delta}$, defined by $I_{\kappa_{n,d}}(\delta, \delta) = 1/n$.

Proof. From standard extreme-value theory (see, e.g., [5, p. 59]), the random variable $\zeta(n, d)/\kappa_{n,d}$ in (7) converges in distribution to the random variable ξ_d . \square

Remark 4.1. *Lemma 4.1 yields the following approximations for the s -moment of $d(\mathbf{u}, \mathbf{R}_n)$ for large n and any given \mathbf{u} :*

$$M_s(d, n, a, r) = \int_{\zeta \geq 0} [(r - a)^2 + 4ar\kappa_{n,d}\zeta]^{s/2} dF_d(\zeta),$$

with $r = \|\mathbf{u}\|$. Explicit expressions are easily obtained for even s . Assuming that $\|\mathbf{u}\| = 1$, this gives in particular the approximations

$$\begin{aligned} \text{var}_2 &= 16a^2 \kappa_{n,d}^2 \text{var}\{\xi_d\} = 16a^2 \kappa_{n,d}^2 [\Gamma(1 + 2/\delta) - \Gamma^2(1 + 1/\delta)], \\ \text{var}_4 &= 64a^2 \kappa_{n,d}^2 \{ (1-a)^4 \text{var}\{\xi_d\} + a^2 \kappa_{n,d}^2 \text{var}\{\xi_d^2\} \\ &\quad + (1-a)^2 a \kappa_{n,d} [\Gamma(1 + 3/\delta) - \Gamma(1 + 1/\delta)\Gamma(1 + 2/\delta)] \}. \end{aligned}$$

for $\text{var}_s = \text{var}\{d^s(\mathbf{u}, \mathbf{R}_n)\}$ when $s = 2$ and $s = 4$, respectively. \triangleleft

The random variables $\zeta(n, d)$ in (7) depend on \mathbf{u} and \mathbf{R}_n , but (18) shows that the dependence in \mathbf{R}_n vanishes asymptotically, so that ξ_d only depends on $\mathbf{u}/\|\mathbf{u}\|$. We hence obtain the following extreme-value approximation of $D_{\mu,s}(\mathbb{P}_a^{[n]})$ for μ spherically symmetric.

Definition 4.1. *Assume that $d \geq 3$ and that μ is spherically symmetric. For any $\mathbf{R}_n \stackrel{d}{\sim} \mathbb{P}_a^{[n]}$, the extreme-value approximation of the (μ, s) -distortion $E_{\mu,s}^s(\mathbf{R}_n)$ is defined by*

$$\widehat{E}_{\mu,s}^s(n; a) = \int_{r \geq 0} \int_{\zeta \geq 0} [(r - a)^2 + 4ar\kappa_{n,d}\zeta]^{s/2} dF_d(\zeta) d\Psi(r), \quad (19)$$

where $\Psi(\cdot)$ is the c.d.f. of $\|U\|$ with $U \stackrel{d}{\sim} \mu$, $F_d(t) = 1 - \exp(-t^\delta)$ with $\delta = (d-1)/2$, and $\kappa_{n,d}$ is the $1/n$ quantile of $\beta_{\delta,\delta}$ defined by $I_{\kappa_{n,d}}(\delta, \delta) = 1/n$. The extreme-value approximation $\widehat{D}_{\mu,s}(\mathbb{P}_a^{[n]})$ of $D_{\mu,s}(\mathbb{P}_a^{[n]})$ is defined by $\widehat{D}_{\mu,s}(\mathbb{P}_a^{[n]}) = \widehat{E}_{\mu,s}^s(n; a)$.

The approximation (19) is derived as follows. Since μ is spherically symmetric, we have $U \stackrel{d}{\sim} r \cdot U^{(d)}$ where $U^{(d)}$ is uniformly distributed on $\mathcal{S}_{d-1}(1)$ and r has the c.d.f. $\Psi(\cdot)$. Since ξ_d in (18) only depends on $U^{(d)}$ and has the c.d.f. $F_d(\cdot)$, the substitution of $(r-a)^2 + 4ar\kappa_{n,d}\zeta(U^{(d)})$ for $d^2(U, \mathbf{R}_n)$ in $E_{\mu,s}^s(\mathbf{R}_n) = \mathbf{E}_\mu\{d^s(U, \mathbf{R}_n)\}$ gives (19). In contrast with Remark 4.1 where \mathbf{u} is fixed, averaging over \mathbf{u} removes the variability (but the means are identical; that is, $\widehat{E}_{\mu,s}^s(n; a) = \mathbf{E}_{\mathbb{P}_a^{[n]}}\{d^s(\mathbf{u}, \mathbf{R}_n)\}$).

For s even, $\widehat{E}_{\mu,s}^s(n; a)$ can be expressed explicitly in terms of moments of $\|U\|$, $M_{\Psi,k} = \mathbf{E}_\mu\{\|U\|^k\} = \int_{r \geq 0} r^k d\Psi(r)$, and moments $\mathbf{E}\{\zeta^k\} = \Gamma(1 + k/\delta)$ of the Weibull distribution. In particular, for $s = 2$ and 4 we get the following extreme-value approximations for the (μ, s) -distortions:

$$\widehat{E}_{\mu,2}^2(n; a) = M_{\Psi,2} - 2a M_{\Psi,1} + a^2 + 4a\kappa_{n,d} M_{\Psi,1} \Gamma(1 + 1/\delta), \quad (20)$$

$$\begin{aligned} \widehat{E}_{\mu,4}^4(n; a) &= M_{\Psi,4} - 4a M_{\Psi,3} + 6a^2 M_{\Psi,2} - 4a^3 M_{\Psi,1} + a^4 \\ &\quad + 8a\kappa_{n,d} \Gamma(1 + 1/\delta) (M_{\Psi,3} - 2a M_{\Psi,2} + a^2 M_{\Psi,1}) \\ &\quad + 16a^2 \kappa_{n,d}^2 M_{\Psi,2} \Gamma(1 + 2/\delta). \end{aligned} \quad (21)$$

Denote by $\widehat{a}^* = \widehat{a}^*(d, n, s)$ the value of a that minimises $\widehat{E}_{\mu,s}^s(n; a)$, which forms an extreme-value approximation of the optimal a^* minimising $D_{\mu,s}(\mathbb{P}_a^{[n]})$. In the next corollary, we give the expressions of $\widehat{a}^*(d, n, 2)$ and $\widehat{E}_{\mu,2}^2(n; \widehat{a}^*)$; the later providing an extreme-value approximation for $\min_a D_{\mu,2}(\mathbb{P}_a^{[n]})$.

Corollary 4.1. *For $d \geq 3$, μ spherically symmetric and $\mathbf{R}_n \stackrel{d}{\sim} \mathbb{P}_a^{[n]}$, we have*

$$\begin{aligned} \widehat{a}^* &= \widehat{a}^*(d, n, 2) = M_{\Psi,1} [1 - 2\kappa_{n,d} \Gamma(1 + 1/\delta)], \\ \widehat{E}_{\mu,2}^2(n; \widehat{a}^*) &= M_{\Psi,2} - (\widehat{a}^*)^2. \end{aligned} \quad (22)$$

For μ uniform on $\mathcal{B}_d(1)$, Figure 12 indicates that $\widehat{a}^*(d, n, 2)$ and $a^*(d, n, 2)$ are practically indistinguishable for $n = 1000$ and $n = 100000$ with $d = 10, \dots, 50$. For the situation considered in Section 3.4 where $U \stackrel{d}{\sim} \mathcal{N}(\mathbf{0}_d, \mathbf{I}_d/d)$, $\widehat{a}^*(d, n, 2)$ is also very close to $a^*(d, n, 2)$ when n is large enough; its evolution as a function of d for $n = 10000$ is visually indistinguishable from that of $a^*(d, n, s)$ on the left panel of Figure 8.

The expressions for $\widehat{a}^* = \widehat{a}^*(d, n, 4)$ and $\widehat{E}_{\mu,4}^4(n; \widehat{a}^*)$ can also be written in analytic form (by finding the roots of a third-degree polynomial), but the expressions are cumbersome.

4.2 Three asymptotic regimes for n growing with d

In view of Lemma 4.1, the asymptotic behaviour of $\kappa_{n,d}$ is the key element in understanding that of $d^2(\mathbf{u}, \mathbf{R}_n)$. For $d = 3$, $\beta_{1,1}$ is uniform on $[0, 1]$ and we simply have $\kappa_{n,3} = 1/n$. For $d > 3$ there is no explicit formula for $\kappa_{n,d}$, but it can easily be computed numerically by solving $I_{\kappa_{n,d}}(\delta, \delta) = 1/n$. For fixed $t \leq 1/2$, $I_t(\delta, \delta)$ decreases as δ increases. Therefore, $\kappa_{n,d}$ is an increasing function of d for any fixed $n \geq 2$ (it is also a decreasing function of n for any fixed d). When n tends to infinity with d we have the following properties.

Proposition 4.1. *For fixed $d \geq 3$, the $1/n$ quantile $\kappa_{n,d}$ of $\beta_{\delta,\delta}$ with $\delta = (d-1)/2$ tends to zero as n tends to infinity. When $d \rightarrow \infty$ and $n = n(d)$ grows with d , we have the following three cases:*

- (i) if $n^{1/d} \rightarrow \infty$, then $\lim_{d \rightarrow \infty} \kappa_{n,d} = 0$;
- (ii) if $n = C\lambda^d (1 + o(1))$ with $\lambda > 1$ and $C > 0$, then

$$\lim_{d \rightarrow \infty} \kappa_{n,d} = \frac{1}{2} \left[1 - \sqrt{1 - 1/\lambda^2} \right]; \quad (23)$$

(iii) if $(\log n)/d \rightarrow 0$, then $\lim_{d \rightarrow \infty} \kappa_{n,d} = \frac{1}{2}$.

Proof. Since $x^{\delta-1}(1-t)^\delta \leq x^{\delta-1}(1-t)^{\delta-1} \leq x^{\delta-1}(1-x)^{\delta-1}$ for $\delta \geq 1$ and all $t \in [0, 1]$ and $x \in [0, t]$, we have

$$\frac{t^\delta(1-t)^\delta}{\delta B(\delta, \delta)} \leq I_t(\delta, \delta). \quad (24)$$

The derivation of an exploitable upper bound is more delicate. Assume that $d \geq 3$ and let $\delta' = \lfloor \delta \rfloor$, the largest integer smaller than or equal to δ . As $n \geq 2$, we are only interested in values of t less than $1/2$. Since $\delta' \leq \delta$, we have $I_t(\delta, \delta) \leq I_t(\delta', \delta')$, which can be calculated explicitly by successive integration by parts. Direct calculations yield the following special case of the well-known relation between the c.d.f. of the beta and binomial distributions:

$$I_t(\delta', \delta') = \sum_{k=0}^{\delta'-1} \binom{2\delta'-1}{k} t^{2\delta'-1-k} (1-t)^k, \quad (25)$$

$$= t^{\delta'} (1-t)^{\delta'-1} \sum_{k=0}^{\delta'-1} \binom{2\delta'-1}{k} \left(\frac{t}{1-t} \right)^{\delta'-1-k}. \quad (26)$$

Using the property $t/(1-t) \leq 1$ for $t \leq 1/2$, with $\sum_{k=0}^{\delta'-1} \binom{2\delta'-1}{k} = 4^{\delta'-1}$, we thus obtain

$$I_t(\delta, \delta) \leq I_t(\delta', \delta') \leq t^{\delta'} [4(1-t)]^{\delta'-1} \leq \frac{1}{2} [4t(1-t)]^{\delta'-1}, \quad t \leq 1/2. \quad (27)$$

Together with (24), this implies, for $n \geq 2$ and $d \geq 3$,

$$\frac{1}{2} \left[1 - \sqrt{1 - (2/n)^{1/(\delta'-1)}} \right] \leq \kappa_{n,d} \leq \frac{1}{2} \left[1 - \sqrt{(1 - 4c_d n^{-1/\delta})_+} \right], \quad (28)$$

where $(x)_+ = \max\{x, 0\}$ and $c_d = [\delta B(\delta, \delta)]^{1/\delta} = 1/4 + (\log d)/(4d) + \mathcal{O}(1/d)$, $d \rightarrow \infty$ (with, moreover, $(4c_d)^\delta < d + 2$ for all $d \geq 2$, implying that the right-hand side of (28) is strictly smaller than $1/2$ for $n \geq d + 2$).

When d is fixed and $n \rightarrow \infty$, or $n^{1/d} \rightarrow \infty$ as $d \rightarrow \infty$, $n^{-1/d} \rightarrow 0$ implying that the right-hand side of (28) tends to zero. Therefore, $\kappa_{n,d} \rightarrow 0$.

When $n = C\lambda^d (1 + o(1))$ with $\lambda > 1$ and $C > 0$ (case (ii)), by taking the limits on left and right hand sides of (28), as $\lim_{d \rightarrow \infty} c_d = 1/4$, we obtain $\lim_{d \rightarrow \infty} \kappa_{n,d} = (1/2) \left[1 - \sqrt{1 - 1/\lambda^2} \right]$.

When $\log n = o(d)$, (case (iii)), $n^{-1/d} \rightarrow 1$ and the left-hand side of (28) tends to $1/2$. \square

The left panel of Figure 9 plots $\kappa_{n,d}$ as a function of d for different n : the continuation of each curve (with n fixed) goes to the limiting value $1/2$ in view of Proposition 4.1-(iii). The bounds in (28) are asymptotically accurate for large n , particularly the upper bound, but lack precision for smaller n . For illustration, only the envelope for $n = 10^3$ is shown.

4.3 μ uniform on the unit sphere $\mathcal{S}_{d-1}(1)$

When $U \stackrel{d}{\sim} \mu$ uniform on $\mathcal{S}_{d-1}(1)$, for any $\mathbf{R}_n \stackrel{d}{\sim} \mathbb{P}_a^{[n]}$ the approximations (20) and (21) become

$$\begin{aligned} \widehat{E}_{\mu,2}(n; a) &= [(1-a)^2 + 4a \kappa_{n,d} \Gamma(1+1/\delta)]^{1/2}, \\ \widehat{E}_{\mu,4}(n; a) &= [(1-a)^4 + 16a^2 \kappa_{n,d}^2 \Gamma(1+2/\delta) + 8a(1-a)^2 \kappa_{n,d} \Gamma(1+1/\delta)]^{1/4}. \end{aligned}$$

For $s = 2$, Corollary 4.1 gives $\widehat{a}^* = \widehat{a}^*(d, n, 2) = 1 - 2\kappa_{n,d}\Gamma(1+1/\delta)$ and $\widehat{E}_{\mu,2}^2(n; \widehat{a}^*) = 1 - (\widehat{a}^*)^2$. The right panel of Figure 9 plots $\widehat{a}^*(d, n, 2) - a^*(d, n, 2)$ as a function of d for different values of n : $\widehat{a}^* - a^* > 0$ and the accuracy of the approximation of a^* by \widehat{a}^* tends to decrease with d and increase with n .

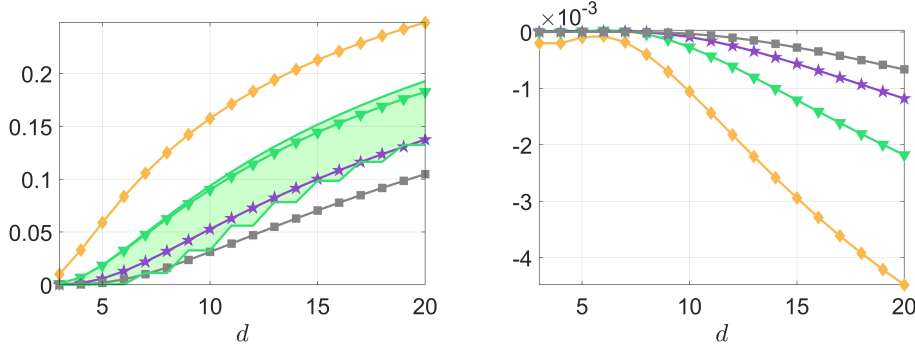


Figure 9: Values of $\kappa_{n,d}$ (left) and of $\widehat{a}^*(d, n, 2) - a^*(d, n, 2)$ (right) as functions of d for different values of n : $n = 10^2$ (♦), $n = 10^3$ (▼), $n = 10^4$ (★) and $n = 10^5$ (■).

The left and right panels of Figure 10 show that the two approximations $\widehat{D}_{\mu,2}(\mathbb{P}_a^{[n]})$ and $\widehat{D}_{\mu,4}(\mathbb{P}_a^{[n]})$ are quite accurate when n is large enough for extreme value theory to be applicable. For large d , convergence to the extreme-value distribution is slow and $\widehat{D}_{\mu,s}^{1/s}(\mathbb{P}_a^{[n]})$ slightly overestimates the true value $D_{\mu,s}^{1/s}(\mathbb{P}_a^{[n]})$.

The left panel of Figure 11 provides another illustration of the accuracy of the estimation, and presents normalised values $n^{1/d} \widehat{D}_{\mu,s}^{1/s}(\mathbb{P}_a^{[n]})$ and $n^{1/d} D_{\mu,s}^{1/s}(\mathbb{P}_a^{[n]})$ as functions of $n = 2^m$, $m = 6, 7, \dots, 20$, for $s = 4$ and $d = 20$, both for $a = 0.75$ fixed and a optimal, i.e., $a^*(d, n, s)$ (the plots with $\widehat{a}^*(d, n, s)$ substituted for $a^*(d, n, s)$ are visually indistinguishable). The value $\widehat{D}_{\mu,s}^{1/s}(\mathbb{P}_a^{[n]})$ approaches $D_{\mu,s}^{1/s}(\mathbb{P}_{a^*}^{[n]})$ for n such that $a^* = a^*(d, n, s) \simeq 0.75$. On the right panel of Figure 11, for each n considered, 100 values of $n^{1/d} E_{\mu,s}(\mathbf{R}_n)$ computed numerically¹ for 100 random point sets $\mathbf{R}_n \stackrel{d}{\sim} \mathbb{P}_{a^*}^{[n]}$ have been added to the plots of $n^{1/d} \widehat{D}_{\mu,s}^{1/s}(\mathbb{P}_{a^*}^{[n]})$ and $n^{1/d} D_{\mu,s}^{1/s}(\mathbb{P}_{a^*}^{[n]})$. The simulations are in perfect adequation with the exact mean value $n^{1/d} D_{\mu,s}^{1/s}(\mathbb{P}_{a^*}^{[n]})$ and indicate that the variability of $E_{\mu,s}(\mathbf{R}_n)$ across quantisers is very small.

The property below shows that the asymptotic behaviour of $\widehat{a}^*(d, n, s)$ when n tends to infinity with d does not depend on s .

Corollary 4.2. *When $n = n(d)$ grows with $d \rightarrow \infty$, we have the following three cases for the limit of $\widehat{a}^*(d, n, s)$:*

- (i) if $n^{1/d} \rightarrow \infty$, then $\lim_{d \rightarrow \infty} \widehat{a}^*(d, n, s) = 1$;
- (ii) if $n = \lambda^d (1 + o(1))$ with $\lambda > 1$, then $\lim_{d \rightarrow \infty} \widehat{a}^*(d, n, s) = \widehat{a}_\lambda^* = \sqrt{1 - 1/\lambda^2}$;
- (iii) if $\log n = o(d)$, then $\lim_{d \rightarrow \infty} \widehat{a}^*(d, n, s) = 0$.

Proof. Definition (19) gives

$$\widehat{E}_{\mu,s}^s(n; a) = \int_{\zeta \geq 0} [(1-a)^2 + 4a\kappa_{n,d}\zeta]^{s/2} dF_d(\zeta),$$

where the Weibull distribution tends to be concentrated at 1 when $d \rightarrow \infty$. This implies that, for any given s , $\lim_{d \rightarrow \infty} \widehat{E}_{\mu,s}^s(n; a) - [(1-a)^2 + 4a\kappa_{n,d}]^{s/2} = 0$, where $\kappa_{n,d}$ has

¹We used 2¹² i.i.d. $U_i \stackrel{d}{\sim} \mu$, which provides an accurate enough estimation of $E_{\mu,s}(\mathbf{R}_n)$; see Remark 2.1.

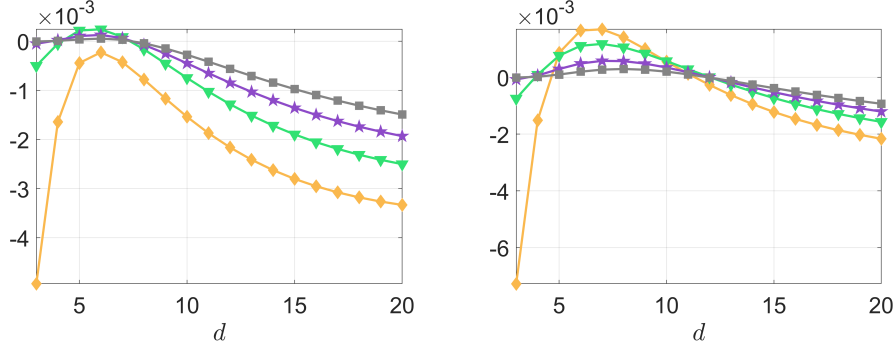


Figure 10: Relative error $1 - \widehat{D}_{\mu,s}^{1/s}(\mathbb{P}_a^{[n]})/D_{\mu,s}^{1/s}(\mathbb{P}_a^{[n]})$ of the approximation of $D_{\mu,s}^{1/s}(\mathbb{P}_a^{[n]})$ (left for $s=2$ and right for $s=4$) based on extreme-value theory, as a function of d for different values of n : $n=10^2$ (\diamond), $n=10^3$ (∇), $n=10^4$ (\star) and $n=10^5$ (\blacksquare); a is the optimal value $a^*(d, n, s)$.

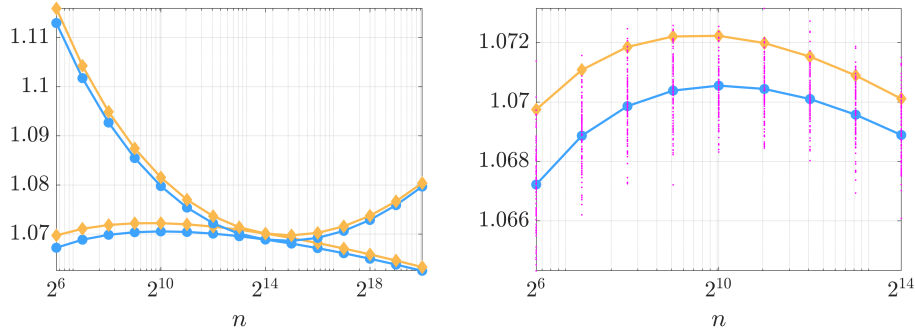


Figure 11: $n^{1/d} \widehat{D}_{\mu,s}^{1/s}(\mathbb{P}_a^{[n]})$ (\diamond) and $n^{1/d} D_{\mu,s}^{1/s}(\mathbb{P}_a^{[n]})$ (\bullet) as functions of n for $s=4$ and $d=20$. Left: $a=0.75$ for top curves and $a=a^*(d, n, s)$ for bottom curves. Right: $a=a^*(d, n, s)$, the values of $n^{1/d} E_{\mu,s}(\mathbf{R}_n)$ computed numerically for 100 random quantisers $\mathbf{R}_n \stackrel{d}{\sim} \mathbb{P}_{a^*}^{[n]}$ are shown as magenta dots.

the limiting behaviour indicated in Proposition 4.1. Therefore, $\lim_{d \rightarrow \infty} \widehat{a}^*(d, n, s) = \lim_{d \rightarrow \infty} 1 - 2\kappa_{n,d}$ does not depend on s and is as indicated above for the three cases considered. \square

On the left panel of Figure 1 we can observe the tendency $a^*(d, n, s) \rightarrow 0$ when d is large but n is not exponentially large compared to d ; on the top-left panel with $d=10$ we see that $a^*(d, n, 1)$ approaches 1 as n increases. The left panel of Figure 3 provides an illustration of case (ii) for $n=2^d$ (i.e., $\lambda=2$) with $s=2, 4$, for which $\widehat{a}_\lambda^* = \sqrt{3}/2 \simeq 0.8660$.

From Lemma 4.1, the same arguments as those leading to Definition 4.1 indicate that, for any $\mathbf{R}_n \stackrel{d}{\sim} \mathbb{P}_a^{[n]}$ the extreme-value approximation of the γ -quantile of the distance c.d.f. $F_n(t; \mathbf{R}_n, \mu)$ is $\widehat{q}_\gamma = \sqrt{(1-a)^2 + 4a\kappa_{n,d}t_\gamma}$, with $t_\gamma = [-\log(1-\gamma)]^{1/\delta}$ the γ -quantile of the Weibull distribution with c.d.f. $F_d(t) = 1 - \exp(-t^\delta)$, $\delta = (d-1)/2$.

The minimum of \widehat{q}_γ with respect to a is obtained for $\widehat{a}_*(d, n, \gamma) = 1 - 2\kappa_{n,d}t_\gamma$. Since $t_\gamma \rightarrow 1$ as $d \rightarrow \infty$, for any fixed γ , $\widehat{a}_*(d, n, \gamma)$ has the same limits as those indicated in Corollary 4.2 for $\widehat{a}^*(d, n, s)$, independently of γ , when $n = n(d) \rightarrow \infty$.

Remark 4.2. Note that $\widehat{q}_\gamma = \widehat{E}_{\mu,2}(n;a)$ for any a when $\gamma = \gamma(d,2) = F_d[\Gamma(1 + 1/\delta)]$, showing that for large n , minimising the expected $(\mu,2)$ -distortion is equivalent to minimising the γ -quantile of the mean distance c.d.f. for

$$\gamma = \gamma(d,2) = 1 - e^{-e^{-\gamma}} + \frac{\pi^2}{6d} e^{-\gamma - e^{-\gamma}} + \mathcal{O}(d^{-2}), \quad d \rightarrow \infty,$$

where γ is Euler's constant and $1 - e^{-e^{-\gamma}} \simeq 0.429624$. This suggests that L_2 -quantisation is roughly equivalent to minimising the median of the distance c.d.f., a phenomenon that can also be observed for other sets than the sphere. \triangleleft

4.4 μ possesses a norm-concentration property

We say that the probability measure μ on \mathbb{R}^d possesses a *norm-concentration property* when it satisfies

$$\text{for all } \epsilon > 0, \quad \mu \{ \|\|U\| - A\| \geq \epsilon \} \leq 2 \exp(-c d \epsilon^2) \quad (29)$$

when $U \sim \mu$, for some $A > 0$ and c a constant not depending on d . A multivariate distribution such that the components of U are independent and sub-Gaussian with zero mean and strictly positive variance satisfies (29), see [12, Th. 3.1.1]. Here we consider distributions that satisfy (29) and are spherically-symmetric, with the uniform distribution in $\mathcal{B}_b(1)$ and the multivariate normal distribution for which $r = \|U\|$ has the density (16) as particular cases. Both satisfy (29) with $A = 1$ and, without any loss of generality we consider measures μ such that $A = 1$ in the following.

We continue to consider random quantisers $\mathbf{R}_n \stackrel{d}{\sim} \mathbb{P}_a^{[n]}$, focusing on the extreme-value approximation $\widehat{D}_{\mu,s}(\mathbb{P}_a^{[n]})$ of the (μ, s) -distortion as defined in Definition 19. When $n = n(d)$ grows with d and μ is simply spherically symmetric, the limiting value of $\widehat{a}^*(d, n, s)$ which minimises $\widehat{D}_{\mu,s}(\mathbb{P}_a^{[n]})$ generally depends on s in cases (i) and (ii) of Corollary 4.2. The next proposition shows that, if μ satisfies (29), the asymptotic behaviour of $\widehat{a}^*(d, n, s)$ remains unchanged from that described in Corollary 4.2.

Proposition 4.2. Assume that $d \geq 3$, that $\mathbb{P} = \mathbb{P}_a^{[n]}$, and that μ is spherically symmetric and satisfies (29). Then, as $d \rightarrow \infty$ with $n = n(d)$ growing accordingly, the limit of $\widehat{a}^*(d, n, s)$ follows the three cases outlined in Corollary 4.2.

Proof. Consider the random variable $T_{n,d} = (r - a)^2 + 4 a r \kappa_{n,d} \zeta$ in (19). The limiting value κ_∞ of the quantile $\kappa_{n,d}$ in the three cases considered is given in Proposition 4.1, and $T_{n,d}$ converges in probability to $T_\infty = (1 - a)^2 + 4 a \kappa_\infty$ when $d \rightarrow \infty$. From (29), for any given $s > 0$ the sequence $\{T_{n,d}^{s/2}\}$ is bounded in L^p for any p and is thus uniformly integrable. Therefore, $\widehat{D}_{\mu,s}(\mathbb{P}_a^{[n]}) \rightarrow T_\infty^{s/2}$, which is minimum for the values of a indicated in Corollary 4.2. \square

To illustrate the above analysis, we consider again two specific cases for μ : uniform distribution in the unit ball $\mathcal{B}_d(1)$, in the small n regime with fixed n and increasing d ; multivariate normal distribution $\mathcal{N}(\mathbf{0}_d, \mathbf{I}_d/d)$, in the exponential regime with $n = 2^d$.

4.4.1 μ is uniform in the unit ball $\mathcal{B}_d(1)$

In the non-asymptotic regime, $\widehat{a}^*(d, n, 2)$ is given by (22) for $s = 2$; for $s = 4$, $\widehat{a}^*(d, n, 4)$ is a root of the third-degree polynomial corresponding to the derivative of (21).

Figure 12 displays the following quantities as functions of d for two values of n : $a^*(d, n, 2)$, its approximation $\hat{a}^*(d, n, 2)$, and $b^*(d, n, 2)$, which minimises $D_{\mu,2}(\mathbb{P}_{0,b}^{[n]})$ (see Section 3.3). The comparative behaviour of $a^*(d, n, 2)$ and $b^*(d, n, 2)$ has already been discussed in Section 3.3; the plots of $a^*(d, n, 2)$ and $\hat{a}^*(d, n, 2)$ are practically indistinguishable.

Figure 13 displays the efficiencies $D_{\mu,s}^{1/s}(\mathbb{P}_a^{[n]})/D_{\mu,s}^{1/s}(\mathbb{P}_{0,b^*}^{[n]})$ as functions of d for $a = a^*(d, n, 2)$ and $a = \hat{a}^*(d, n, 2)$. These efficiencies are quasi indistinguishable, and $\mathbb{P}_{a^*}^{[n]}$ and $\mathbb{P}_{\hat{a}^*}^{[n]}$ both outperform $\mathbb{P}_{0,b^*}^{[n]}$ for the values of n and d considered. Additionally, $\mathbb{P}_{0,b^*}^{[n]}$ significantly outperforms $\mathbb{P}_{0,1}^{[n]}$; see Figure 4 in Section 3.3.

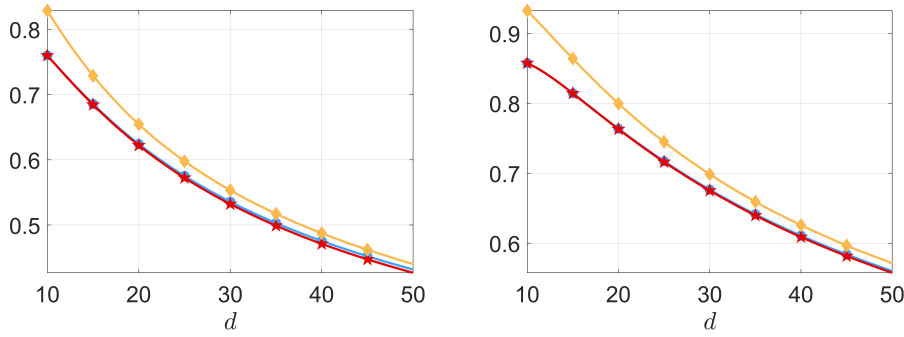


Figure 12: $a^*(d, n, 2)$ (\bullet), $\hat{a}^*(d, n, 2)$ (\star) and $b^*(d, n, 2)$ (\diamond) as functions of d for $n = 1000$ (left) and $n = 100000$ (right).

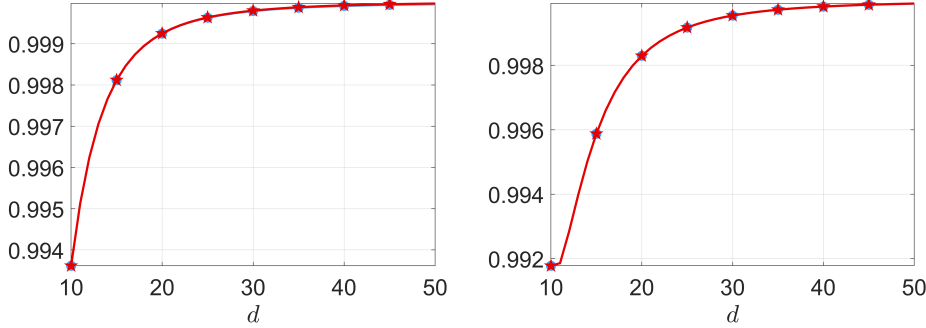


Figure 13: Efficiencies $D_{\mu,s}^{1/s}(\mathbb{P}_a^{[n]})/D_{\mu,s}^{1/s}(\mathbb{P}_{0,b^*}^{[n]})$ as functions of d : $a = a^*(d, n, 2)$ (\bullet), $a = \hat{a}^*(d, n, 2)$ (\star); $n = 1000$ (left) and $n = 100000$ (right).

4.4.2 μ is normal $\mathcal{N}(\mathbf{0}_d, \mathbf{I}_d/d)$

We noticed in Section 3.4 that $D_{\mu,s}(\mathbb{P}_{a^*}^{[n]}) < D_{\mu,s}(\mu_{\sigma^*}^{[n]})$ for $n \lesssim n_0 \lambda_0^d$ for some n_0 and λ_0 , where $a^* = a^*(d, n, s)$ and σ^* respectively minimise $D_{\mu,s}(\mathbb{P}_a^{[n]})$ and $D_{\mu,s}(\mu_{\sigma}^{[n]})$. Here we investigate the behaviour of $D_{\mu,s}(\mathbb{P}_a^{[n]})$ for other choices of a in a similar asymptotic regime where n grows exponentially fast with d .

Given that $M_{\psi,1} = \mathbf{E}\{\|U\|\} \rightarrow 1$ and $\text{var}\{\|U\|\} \rightarrow 0$ as $d \rightarrow \infty$ when $U \sim \mu$, we analyse the following cases for a . (i) Uniform distribution on $\mathcal{S}_{d-1}(1)$: we consider $a = \tilde{a}^*(d, n, s)$ which minimises $D_{\mu,s}^{1/s}(\mathbb{P}_a^{[n]})$ for $\tilde{\mu}$ uniform on $\mathcal{S}_{d-1}(1)$, as

discussed in Section 3.1. (ii) Scaled uniform distribution: we also consider $a = M_{\psi,1}\tilde{a}^*(d,n,s)$, obtained when $\tilde{\mu}$ is uniform on $\mathcal{S}_{d-1}(M_{\psi,1})$. As we consider the asymptotic regime $n = 2^d$, we additionally examine (iii) the limiting value $\widehat{a}_\lambda^* = \sqrt{3}/2$ from Corollary 4.2-(ii); (iv) the value $\widehat{a}^*(d,n,s)$, which minimises $\widehat{E}_{\mu,s}^s(n;a)$ given by (19), where the quantile $\kappa_{n,d}$ is replaced by its asymptotic value $(1/2)(1 - \sqrt{3}/2)$.

Figure 14 (left) displays $\sigma^*(d,n,s)$, $a^*(d,n,s)$, $\tilde{a}^*(d,n,s)$ and $M_{\psi,1}\tilde{a}^*(d,n,s)$ as functions of d for $s = 4$, together with \widehat{a}_λ^* (indicated by an horizontal line) and $\widehat{a}^*(d,n,s)$. The right panel in the same figure shows the efficiency of the optimal normal distribution μ_{σ^*} compared to \mathbb{P}_a uniform on $\mathcal{S}_{d-1}(a)$, that is, $D_{\mu,s}^{1/s}(\mathbb{P}_a^{[n]})/D_{\mu,s}^{1/s}(\mu_{\sigma^*}^{[n]})$, for the five choices of a considered: \mathbb{P}_a performs better than μ_{σ^*} (for $d \geq 4$ when $a = M_{\psi,1}\tilde{a}^*(d,n,s)$). Note that the efficiencies for \widehat{a}_λ^* (purple triangles) and $a^*(d,n,s)$ (blue dots) almost coincide for $d \geq 5$.

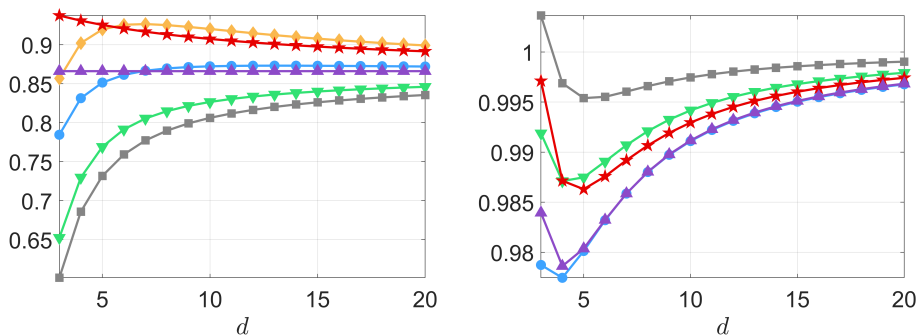


Figure 14: Left: $\sigma^*(d,n,s)$ (\blacklozenge), $a^*(d,n,s)$ (\bullet), $\tilde{a}^*(d,n,s)$ (\blacktriangledown), $M_{\psi,1}\tilde{a}^*(d,n,s)$ (\blacksquare), $\widehat{a}_\lambda^* = \sqrt{3}/2$ (\blacktriangle) and $\widehat{a}^*(d,n,s)$ (\blackstar) as functions of d . Right: efficiencies $D_{\mu,s}^{1/s}(\mathbb{P}_a^{[n]})/D_{\mu,s}^{1/s}(\mu_{\sigma^*}^{[n]})$ as functions of d for the choices of a indicated on the left panel ($n = 2^d$, $s = 4$).

Remark 4.3. From Corollary 4.2 and Proposition 4.2, all quantities $a^*(d,n,s)$, $\tilde{a}^*(d,n,s)$, $M_{\psi,1}\tilde{a}^*(d,n,s)$ and $\widehat{a}^*(d,n,s)$ tend to $\widehat{a}_\lambda^* = \sqrt{3}/2$ when $d \rightarrow \infty$. Our numerical results suggest that, in the considered asymptotic regime, $\sigma^*(d,n,s)$ also converges to the limiting value $\widehat{a}_\lambda^* = \sqrt{3}/2$. However, a rigorous theoretical analysis is still required to confirm this observation. The same is true for the asymptotic behaviour of $b^*(d,n,s)$ in the optimised quantiser $\mathbb{P}_{0,b^*}^{[n]}$ when μ is uniform in $\mathcal{B}_d(1)$. From (6) in Proposition 2.1, we have to analyse the behaviour of $d(\mathbf{u}, \mathbf{R}_n) = \min_{i=1,\dots,n} [(\|\mathbf{u}\| - R_i)^2 + 4\|\mathbf{u}\|R_i\zeta_i]$ when $n \rightarrow \infty$, where the random variables R_i are ζ_i are i.i.d. and mutually independent, with $\zeta_i \stackrel{d}{=} \beta_{\delta,\delta}$. The assumption that $R = \|\mathbf{X}\|$ with the probability measure \mathbb{P} of X satisfying a norm-concentration property like (29) does not directly imply an extreme-value property for $d(\mathbf{u}, \mathbf{R}_n)$. The cases where $\mathbb{P} = \mathbb{P}_a$ (uniform distribution on $\mathcal{B}_d(a)$) and $\mathbb{P} = \mu_\sigma$ (multivariate normal distribution) already pose significant challenges. \triangleleft

5 Conclusions

We have demonstrated that, for a spherically symmetric measure μ in \mathbb{R}^d , unless the sample size n is extremely large, a random quantiser uniformly distributed on a sphere of suitable radius can significantly outperform a random quantiser

whose distribution follows the asymptotic limit predicted by Zador’s theorem. The optimal radius can be determined numerically by minimising a triple integral, which can be evaluated with arbitrary precision. Additionally, an approximation of the optimal radius is available, derived from extreme-value theory. Since the variability of the distortion for such random quantisers rapidly diminishes as n increases, this approach is highly practical for constructing high-performance quantisers.

While the restriction to spherically symmetric distributions may appear limiting, it provides a robust foundation for broader applications. For instance, quantising the uniform measure on the d -dimensional hypercube $[-1, 1]^d$ presents a compelling and challenging problem, particularly in space-filling design for computer experiments (see, e.g., [10]). While greedy quantisation offers an attractive approach for the incremental construction of designs in low dimensions [6, 7], it becomes computationally infeasible for large d . In such cases, recent results from [8] allow the uniform measure to be approximated by a spherically symmetric distribution. Similarly, one can consider random quantisers distributed according to a product measure, which can itself be approximated by a spherically symmetric distribution. Preliminary findings then suggest that quantisers distributed on the vertices of a smaller hypercube exhibit promising performance, paving the way for further advances in this direction.

References

- [1] N. Alon and J.H. Spencer. *The Probabilistic Method*. Wiley, 2000. Second edition.
- [2] K.-T. Fang, S. Kotz, and K.W. Ng. *Symmetric Multivariate and Related Distributions*. Chapman and Hall/CRC, 1990.
- [3] W. Feller. *An Introduction to Probability Theory and Its Applications, vol. 2*. Wiley, New York, 1971. Second edition.
- [4] S. Graf and H. Luschgy. *Foundations of Quantization for Probability Distributions*. Springer, Berlin, 2000.
- [5] S. Kotz and S. Nadarajah. *Extreme Value Distributions: Theory and Applications*. Imperial College Press, 2000.
- [6] H. Luschgy and G. Pagès. Greedy vector quantization. *Journal of Approximation Theory*, 198:111–131, 2015.
- [7] A. Nogales Gómez, L. Pronzato, and M.-J. Rendas. Incremental space-filling design based on coverings and spacings: improving upon low discrepancy sequences. *Journal of Statistical Theory and Practice*, 15(4):77, 2021.
- [8] J. Noonan and A. Zhigljavsky. *High-Dimensional Optimization: Set Exploration in the Non-Asymptotic Regime*. Springer, 2024.
- [9] G. Pagès. A space quantization method for numerical integration. *Journal of Computational and Applied Mathematics*, 89(1):1–38, 1997.
- [10] L. Pronzato and W. Müller. Design of computer experiments: space filling and beyond. *Statistics and Computing*, 22:681–701, 2012.
- [11] L. Pronzato and A.A. Zhigljavsky. Quasi-uniform designs with asymptotically optimal and near-optimal uniformity constant. *Journal of Approximation Theory*, 294(105931), 2023.

- [12] R. Vershynin. *High-Dimensional Probability: An Introduction with Applications in Data Science*. Cambridge University Press, 2018.
- [13] P.L. Zador. Asymptotic quantization error of continuous signals and the quantization dimension. *IEEE Trans. Inform. Theory*, 28:139–149, 1982.